

Deorphanizing Caspase-3 and Caspase-9 Substrates In and Out of Apoptosis with Deep Substrate Profiling

Luam E. Araya,[§] Ishankumar V. Soni,[§] Jeanne A. Hardy, and Olivier Julien*Cite This: *ACS Chem. Biol.* 2021, 16, 2280–2296

Read Online

ACCESS |



Metrics & More

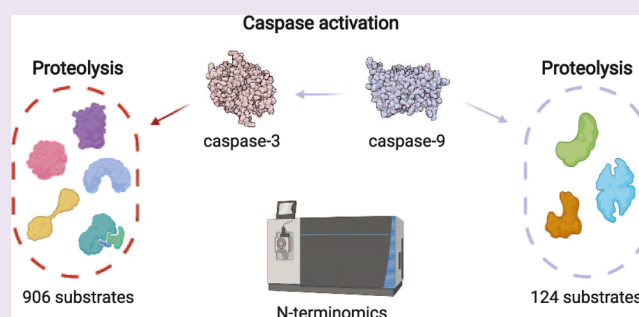


Article Recommendations



Supporting Information

ABSTRACT: Caspases are a family of enzymes that regulate biological processes such as inflammation and programmed cell death, through proteolysis. For example, in the intrinsic pathway of apoptosis, cell death signaling involves cytochrome *c* release from the mitochondria, which leads to the activation of caspase-9 and eventually the executioners caspase-3 and -7. One key step in our understanding of these proteases is to identify their respective protein substrates. Although hundreds of substrates have been linked to caspase-3, only a small handful of substrates have been reported for caspase-9. Employing deep profiling by subtiligase N-terminomics, we present here an unbiased analysis of caspase-3 and caspase-9 substrates in native cell lysates. We identified 906 putative protein substrates associated with caspase-3 and 124 protein substrates for caspase-9. This is the most comprehensive list of caspase substrates reported for each of these proteases, revealing a pool of new substrates that could not have been discovered using other approaches. Over half of the caspase-9 substrates were also cleaved by caspase-3, but often at unique sites, suggesting an evolved functional redundancy for these two proteases. Correspondingly, nearly half of the caspase-9 cleavage sites were not recognized by caspase-3. Our results suggest that in addition to its important role in activating the executioners, the role of caspase-9 is likely broader and more complex than previously appreciated, which includes proteolysis of key apoptotic substrates other than just caspase-3 and -7 and involvement in non-apoptotic pathways. Our results are well poised to aid the discovery of new biological functions for these two caspases.



INTRODUCTION

Caspases are a family of cysteine aspartyl proteases involved in cell fate, most notably as being key drivers of apoptosis and pyroptosis.^{1,2} They also participate in non-apoptotic biological processes, such as tissue differentiation,³ cell proliferation,⁴ and neurodegeneration.⁵ Caspases cleave almost exclusively C-terminal to aspartic acid residues, though each caspase has its own highly tuned substrate specificity.^{6,7} There are 12 human caspases, most of which can be classified as initiator (caspase-2, -8, -9, and -10), executioner (caspase-3, -6, and -7), or inflammatory (caspase-1, -4, -5, and -12), which indicate their role in cell death,⁸ while caspase-14 is known to play a role in terminal differentiation of epidermal keratinocytes.⁹ In this study, we focus our attention on one executioner, caspase-3, and one initiator, caspase-9. The outcomes from our investigation reveal new roles for both caspases and deorphanize many apoptotic substrates.

Caspase-9 is an initiator caspase that functions upstream of caspases-3/-7. In the intrinsic apoptotic pathway, intracellular injury (such as radiation, chemical insults, or growth factor withdrawal) leads to cleavage of BH3-interacting domain death agonist (BID), triggering a signaling cascade which releases cytochrome *c* from the mitochondria into the cytoplasm prompting association with apoptotic protease activating

factor-1 (Apaf1) to form the apoptosome (Figure 1).¹⁰ Procaspase-9 binds to the apoptosome and is activated. Activated caspase-9 then cleaves procaspases-3 and -7 at the intersubunit linker between the large and small subunits, activating both caspases.^{11,12} Procaspase-3 can also be activated via the extrinsic apoptotic pathway. In the extrinsic pathway, pro-apoptotic signals bind to extracellular receptors, leading to the formation of the death-induced signaling complex (DISC). Oligomerization and autocatalytic activation of the initiator caspase-8 occur on the DISC. Once activated, caspase-8 can directly activate procaspase-3 by cleavage of the intersubunit linker or indirectly stimulate caspase-3 activation by cleaving BID and inducing caspase-9.¹⁴

Knowledge of substrates that caspases can cleave is extensive and yet is still incomplete. Some caspases, including caspase-3 and -7, have hundreds of known substrates.^{13–16} In contrast,

Received: June 15, 2021

Published: September 23, 2021



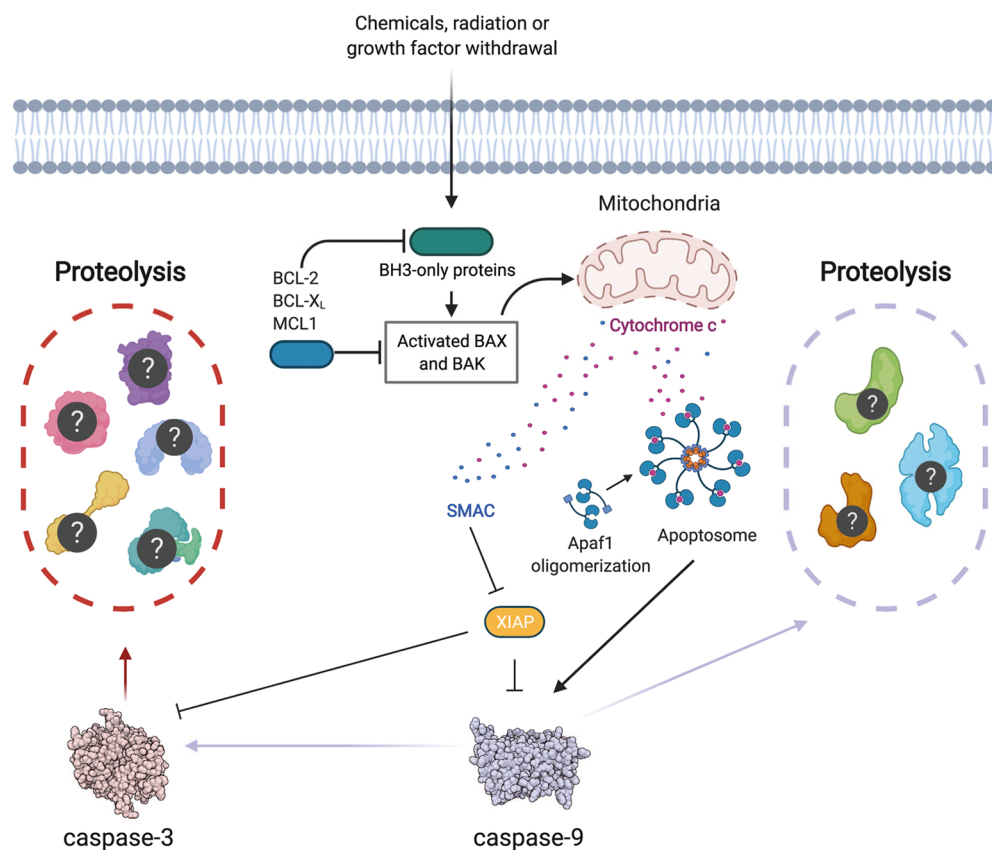


Figure 1. Role of caspase-3 and caspase-9. In healthy cells, cytochrome *c* is mostly restrained to the mitochondria, and an X-linked inhibitor of apoptosis protein (XIAP) blocks caspase function. During apoptosis, the intrinsic pathway is activated by stresses (e.g., radiation, chemical insults, and growth factor withdrawal). This leads to the transcriptional repression of anti-apoptotic proteins, such as BCL-2, BCL-X, and MCL1, and to the activation of BH3-only proteins, which will in turn activate BAX and BAK. This causes cytochrome *c* (pink) and SMAC (blue) (second mitochondria-derived activator of caspase) release from the mitochondria. SMAC interacts with XIAP to prevent caspases inhibition. The cytochrome *c* associates with apaf1, leading to the formation of the apoptosome, ultimately activating caspase-9. The main established role of the initiator caspase-9 (PDB: 1JXQ) is to activate the executioner caspase-3 (PDB: 1QX3). In this study, we address the specificity of caspase-3 and caspase-9 and report their unique set of respective protein substrates.

little is known about the substrates of caspase-9, other than downstream procaspase-3 and -7 proteolysis. In fact, procaspase-6, which is highly homologous to procaspase-3 and -7, and often likewise classified as an executioner, is not directly activated by caspase-9.^{17–19} The first non-procaspase substrate of caspase-9 identified was vimentin,²⁰ which was determined to be cleaved in apoptotic cells. Since then, there have been just six other substrates identified: semaphorin 7A,²¹ SNX1 and SNX2,²² major vault protein,²³ HDAC7,²⁴ and RING2 (also known as RING1B).²⁵

Several methods have been developed over the years to study proteolysis in complex mixtures: subtiligase N-terminomics,²⁶ COFRADIC,²⁷ TAILS,²⁸ and CHOPS.²⁹ COFRADIC and subtiligase N-terminomics,³⁰ in particular, have been extensively used to study caspases. Subtiligase N-terminomics takes advantage of the enzyme subtiligase, an engineered subtilisin enzyme capable of ligating a peptide ester tag to the N-termini of proteins. This technology is useful in determining proteolytic substrates as >80% of the N-termini of mammalian proteins are naturally acetylated,³¹ so subtiligase predominantly ligates peptide ester tags to the neo N-termini created by proteolysis. Thus, subtiligase N-terminomics is a powerful technique to detect cleaved proteins in the complex mixture. This method can be employed in either a forward or a reverse mode. Each mode has its own benefits. Forward N-

terminomics (or *in cellulo*) involves inducing a biological process, such as apoptosis, in cells or tissues to generate cleavage products. However, the identification of the proteases responsible for the proteolytic activity is usually unknown. In reverse N-terminomics (or *in vitro*), a native lysate is incubated with an enzyme to generate cleavage products. This experiment generates cleavages which can be attributed to the added enzyme, but their biological roles are not explicitly revealed.

Subtiligase N-terminomics has been utilized to discover substrates for many human caspases, using both forward and reverse methods. The forward mode has been used to study cell death pathways, which led to the creation of the DegraBase,¹⁵ a repository of cleaved substrates in both healthy and apoptotic cells. The reverse mode has been used to profile substrates of caspases-1, 4, and -5,³² caspase-2 and -6,³³ caspase-7,³⁴ and caspase-3, -7, and -8, but analyzed substrates were limited to those observed under apoptotic conditions in prior forward N-terminomics analysis.¹⁶ These types of analyses have identified critical substrates and opened important new fields of research, such as the discovery of gasdermin D (GSDMD),³² interdomain cleavage of which was found to be sufficient to trigger pyroptosis.^{35–37} Reverse N-terminomics of caspase-9 was performed more than a decade ago, however, no apoptotic substrates were identified,¹⁶ perhaps due to the lower sensitivity of mass spectrometers at

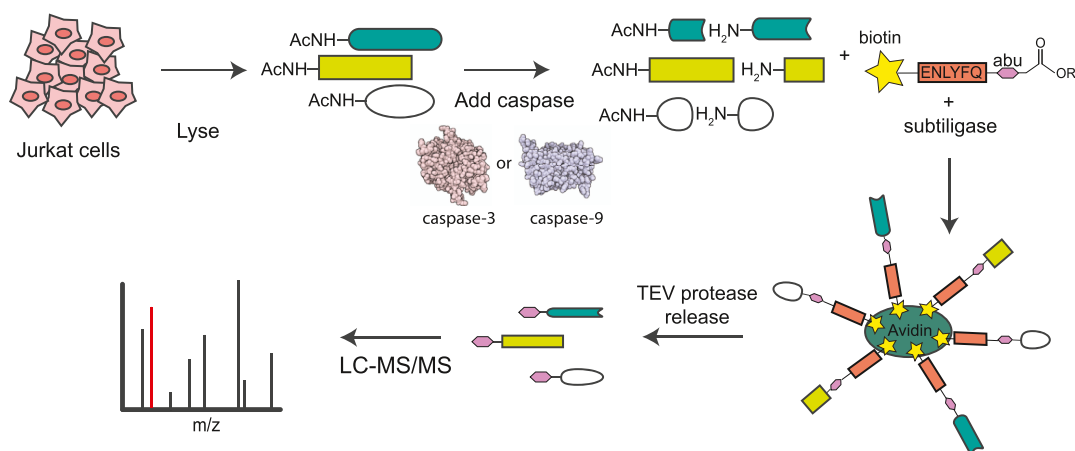


Figure 2. Deep substrates profiling workflow used to deorphanize caspase-3 and -9 substrates. Subtiligase N-termini enrichment was used to label and capture caspase substrates in Jurkat cell lysates. This reverse N-terminomics workflow involves lysing cells in a buffer containing endogenous protease inhibitors, subsequent incubation with either active caspase-3 or -9, enzymatic substrate labeling with a biotin tag at the N-termini, enrichment on agarose beads, trypsinization, and TEV cleavage to release peptides from the beads. The eluted peptides can then be analyzed via LC–MS/MS. Key to this method is the use of a biotin tag featuring a non-standard residue engineered at the TEV cleavage site (ENLYFQ) with a unique mass, abu, which will remain on the N-termini of proteolytic cleavage sites generated in the lysate, allowing unambiguous identification of caspase cleavage sites. Adapted from ref 112.

that time, although a few caspase-9 substrates are known,^{20–25} suggesting that other key substrates remain to be identified.

It is abundantly clear that caspases play major controlling roles in many cell death pathways. The designations as apoptotic initiator (upstream) and executioner (downstream) caspases were provided over two decades ago when the molecular underpinnings of apoptosis began to be reported, and little was known about other mechanisms of cell death.³⁸ During the ensuing decades, a great deal about cell death pathways has been uncovered.^{38–40} In addition, tremendous advances in mass spectrometry and biotechnology methods available to assess protease substrates have been developed.^{29,41–43} This convergence makes possible to address the roles of individual caspases more systematically and more comprehensively and to understand the complex network of interactions in various pathways of cell death. Thus, the goal of this study has been to assess, using the most sensitive cutting-edge approaches, the interplay, redundancy, and substrate pool of one initiator caspase, caspase-9, and one executioner, caspase-3, to distinguish the roles of each caspase in the myriad of cellular pathways. We present here the most comprehensive data sets of caspase-3 and caspase-9 substrates to date. Importantly, we found more than 50 caspase-9 cleavage sites that are not cleaved by caspase-3, suggesting a unique role of caspase-9 in addition to its known canonical role for activating the executioner caspases, caspase-3 and -7.

RESULTS

We report 906 and 124 potential protein substrates targeted by caspase-3 and caspase-9, respectively. These substrates were observed using a subtiligase-based reverse N-terminomics enrichment method (Figure 2). For the analyses of caspase-3 and -9 substrates to play the intended role in providing insights into their respective functions, it is critical that we assess the proteolysis of these caspases in a native environment (substrates folded and interactions maintained), while inhibiting activation of endogenous proteases.^{33,34}

Using reverse N-terminomics, the activities of caspase-3 and -9 were assessed and optimized in Jurkat lysates (Figures S1

and S2). The general schematic diagram of reverse N-terminomics is shown (Figure 2). During cell lysis, background proteolysis was minimized by the addition of protease inhibitors including iodoacetamide which attenuates the activity of endogenous cysteine proteases such as caspases and cathepsins. Dithiothreitol was subsequently supplemented to neutralize excess iodoacetamide, prior to adding purified caspase. In addition, extra precautions were taken for the initiator caspase-9 assay. Jurkat JMR, a caspase-9 deficient cell line,⁴⁴ was used to ensure the measurement of exogenously added caspase-9-cleaved substrates only. To ensure that the executioners caspase-3/-7 were fully inhibited and not contributing to the observed cleavage,¹⁸ Ac-DEVD-fmk was added to the lysate (Figure S1). Subtiligase and biotin ester peptide tag were then added to label the newly generated N-termini of the cleaved products.⁴³ Biotinylated protein fragments were then captured on neutravidin beads, trypsinized, and released by tobacco etch virus (TEV) cleavage. The N-terminomics labeling and capturing efficiency were measured (Figure S3). The eluted peptides were then identified using tandem mass spectrometry (LC–MS/MS) (Figure 2). Importantly, the peptides that have been labeled with the biotin ester peptide tag and released by TEV retain a nonstandard amino acid, aminobutyric acid (abu), that allows for unambiguous identification of proteolytic products and precise location of the cleavage sites.

Caspase-3 and -9 Cleave New and Expected Apoptotic Substrates, Enabling Deorphanization.

Prior subtiligase N-terminomics analysis for caspase-3 observed 180 substrates linked to apoptosis, whereas no substrates were found for caspase-9.¹⁶ This is possibly due to the low intrinsic activity of caspase-9 and the lower sensitivity of the mass spectrometers used in prior N-terminomics assessments. Thus, all caspase-9 substrates known have been reported via individual biological investigations.

In our N-terminomics analyses across two biological replicates, we found 1126 cleavage sites featuring an aspartate at P1 position (P1 = D) in 906 proteins for caspase-3 (1.2 cleavage sites per protein) and 137 cleavage sites in 124

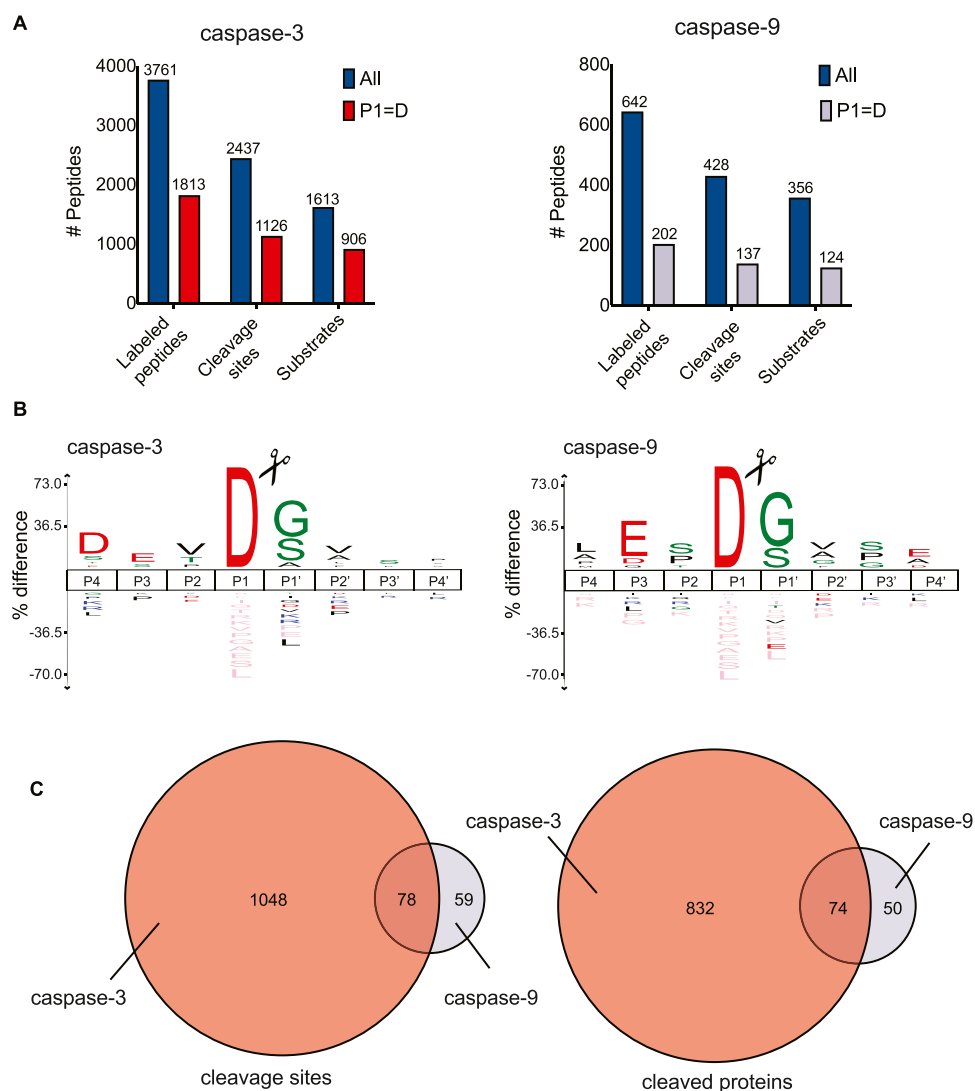


Figure 3. Caspase-3 and -9 substrate discovery. (A) We identified 906 caspase-3 protein substrates (1126 peptides featuring an aspartate at P1 position) and 124 caspase-9 protein substrates (137 peptides featuring an aspartate at P1 position). Some of these substrate proteins are cleaved at multiple sites. (B) IceLogo revealed a clear DEVD↓(G/S/A) motif for caspase-3 and an LESD↓(G/S) motif for caspase-9. (C) Venn diagram shows the overlap between the peptide cleavage sites found in caspase-3 (red) and caspase-9 (gray), showing a set of cleavage sites unique to caspase-9.

proteins (1.1 cleavage sites per protein) for caspase-9 (Figure 3A). The reproducibility between each replicate is presented in Figure S4. The caspase-3 reverse N-terminomics experiments exhibited a P1 = D cleavage in 46% of its labeled N-termini (1126 out of 2437), while the caspase-9 experiment exhibited 32% (137 out of 428) (Figure 3A). This is significantly higher than that found in non-treated cell lysate, where we typically observe 6.5% of N-termini featuring a P1 = D,¹⁵ confirming strong caspase substrate proteolysis induced by the addition of exogenous caspase.

We then aligned each P1 = D peptide from the caspase-3 and caspase-9 data sets to determine the specificity of each protease in human cell lysates, where we anticipate that potential substrates are intact and properly folded (Figure 3B).⁴⁵ The caspase-3 cleavage sites revealed a clear DEVD↓(G/S/A) cleavage motif for amino acids P4–P1↓(P1'),⁴⁶ (Figure 3B) as expected.⁴⁷ The full list of cleavage sites recognized shows considerably greater breadth of recognized sequences than may be reflected in the sequence logo, suggesting that context of the cleavage site, in addition to

the sequence, is critical to substrate recognition (Supplemental File S1). The caspase-9 cleavage sites on the other hand revealed a LESD↓(G/S) cleavage motif for P4–P1↓(P1') (Figure 3B), similar to its reported cleavage specificity for P4–P1↓ as LEHD.⁷ More importantly, there is no evidence of a DEVD cleavage site motif, indicating any DEVDase activity has been fully blocked by the Ac-DEVD-fmk inhibitor (Figure S1). Thus, these results (Figure 3B) strongly suggest that we succeeded in inducing selective caspase proteolysis in each of our caspase-3 and caspase-9 experiments, with no or limited contamination from other activated caspases.

To determine which substrates have already been previously observed in apoptosis, we compared our results with the DegraBase, a repository containing >6000 unique N-termini (>1700 caspase cleavage sites) identified in subtiligase-based N-terminomics of cells undergoing apoptosis.¹⁵ Derived from previous studies, the DegraBase includes the list of proteolytic substrates from many different inducers of apoptosis, including etoposide, staurosporine (STS), TRAIL, bortezomib, and doxorubicin. This important resource does not, however,

Table 1. Caspase-3 and Caspase-9 N-Terminomics Substrates Selected for Deep Interrogation^a

uniprot ID	protein name	cleavage site (P1 = D)	casp3	casp9	DegraBase	localization
RECQ5	ATP-dependent DNA helicase Q5	GEED ⁸⁰⁹ ↓GAGG		+		C
NUP43	nucleoporin Nup43	LDSD ⁵⁸ ↓GGFE		+		N
RN126	E3 ubiquitin–protein ligase RNF126	LFHD ²⁵³ ↓GCIV		+		C
GSDMD	gasdermin-D	DAMD ⁸⁷ ↓GQIQ FLTD ²⁷⁵ ↓GVPA	+		+	C
MFN2	mitofusin-2	DMID ⁴⁹⁹ ↓GLKP	+			M
RNF4	E3 ubiquitin–protein ligase RNF4	DHAD ⁸⁹ ↓SCVV ICMD ¹³⁷ ↓GYSE	+			N, C
PAK2	serine/threonine-protein kinase PAK 2	VGFD ⁸⁹ ↓AVTG PEKD ¹⁴⁸ ↓GFPS	+		+	C
PARN	poly(A)-specific ribonuclease PARN	EQTD ⁵⁹⁵ ↓SCAE	+	+		N, C
ATX2L	ATXN2L	DIVD ¹⁸¹ ↓TMVF LESD ²⁴⁶ ↓MSNG KEVD ⁵⁸⁴ ↓GLLT	+		+	C, CM
RING1	E3 ubiquitin–protein ligase RING1	VSSD ¹⁸⁹ ↓SAPD SAPD ¹⁹³ ↓SAPG	+	+	+	N

^aNote: Complete data sets available online in [Supplemental File S1](#). N = nucleus, C = cytoplasm, CM = cell membrane, M = mitochondrion.

identify which protease is responsible for each cleavage event. By cross-referencing our substrates with the DegraBase, we found that many of the caspase-3 and -9 substrates identified are cleaved during apoptosis ([Supplemental File S1](#)). We can now deorphanize these proteolytic events, linking them to their respective caspases. We found that 577 cleavage sites from caspase-3 (51% of observed cleavages) and 52 cleavage sites from caspase-9 (38% of observed cleavages) had not been previously identified in the DegraBase. We also looked for new substrates that were not previously reported in the DegraBase. We found 257 new caspase-3 and 20 new caspase-9 substrates ([Supplemental File S1](#)). This suggests that these new substrates of caspase-3 and -9 may be present at low abundance or play roles in pathways other than apoptosis.

Comparing the results obtained in these experiments, 43% of the cleavage sites (and 40% of the substrates) observed in the caspase-9 reverse N-terminomics experiment were not observed in the caspase-3 experiment ([Figure 3C](#)). This suggests that many of the substrates and the cleavage sites observed in the caspase-9 reverse experiments are unique to caspase-9, especially considering that caspase-3 is much more active ($k_{\text{cat}}/K_m = 7.6 \times 10^5 \text{ M}^{-1} \text{ s}^{-1}$)⁴⁸ than caspase-9 ($k_{\text{cat}}/K_m = 3.3 \times 10^3 \text{ M}^{-1} \text{ s}^{-1}$).⁴⁹ Furthermore, we observed none of these caspase-9 cleavages in either of the two replicate experiments of caspase-3 N-terminomics. These results are further evidenced by our subsequent characterization (see below).

The distribution of subcellular localization of caspase-3 and -9 substrates is similar, with the majority of substrates being localized to either the cytoplasm or the nucleus ([Figure 5SA](#)). Our N-terminomics method is less suited to detect secreted and membrane proteins, which likely contributes to their lower appearance in our data sets. Within the caspase-3 data set, 49% of the substrate proteins have been reported to be present in the cytoplasm, 48% in the nucleus, 6% in the mitochondria, 7% in the endoplasmic reticulum, 7% in the cell membrane, 4% in other organelles, and 2% were reported to be secreted. A number of substrate proteins have been reported in more than one subcellular location. Within the caspase-9 data set, 47% of substrate proteins were found in the cytoplasm, 55% in the nucleus, 1% in the mitochondria, 6% in the endoplasmic reticulum, 7% in the cell membrane, 4% in other organelles,

and 2% were found to be secreted. Compared to the proteome, there is a higher proportion of proteins localized in the nucleus or cytoplasm (50% in caspase data sets and 25% in proteome), with lower representation of other subcellular locations (1–10% in data sets and 5–15% in proteome).

We also carried out a Reactome⁵⁰ pathway analysis to identify cellular pathways enriched in our data sets. Across both data sets, pathways with the p-values (caspase-3 and caspase-9) below 5.0×10^{-2} were related to mRNA splicing [4.21×10^{-7} (38 substrates), 5.25×10^{-6} (11 substrates)], RNA metabolism [1.38×10^{-7} (95 substrates), 2.30×10^{-5} (11 substrates)] and SUMOylation of proteins [4.04×10^{-5} (32 substrates), 1.25×10^{-2} (six substrates)], including the expected enrichment of proteins associated with apoptosis ([Figure 5SB,C](#)). The complete pathway analysis results are presented in [Supplemental File S1](#). We observed more enrichment for notch-HLH transcription [5.42×10^{-4} (9 substrates)] and HIV infection pathways [1.26×10^{-3} (35 substrates)] in the caspase-3 but not in the caspase-9 data set. For caspase-9, we saw enrichment for mitotic prometaphase [1.85×10^{-3} (eight substrates)], Rho GTPase signaling [3.13×10^{-3} (12 substrates)] and membrane trafficking [3.60×10^{-3} (15 substrates)]. Broadly, we observed enrichment of pathways often found in prior caspase N-terminomics analyses.^{26,33}

We also extracted the location of the caspase cleavage sites from the secondary structure of each substrate, if available ([Figure S6](#)). As expected, the majority of the caspase cleavage sites occur in loop or disordered regions (58% for caspase-3 and 65% for caspase-9), but proteolysis also is observed in regions of α -helices (31% for caspase-3 and 23% for caspase-9) and β -sheets (11% for caspase-3 and 12% for caspase-9) suggesting that local unfolding may also be involved in substrate recognition. We further compared our results to previously published machine learning algorithms used to predict caspase cleavage sites in the human proteome based on protein surface accessibility and secondary structure.⁵¹ Overall, almost all observed cleavage sites reported here scored above the average aspartate site found in the proteome ([Figure S7](#)), supporting the predictions.

From the N-terminomics results, we individually examined each substrate and selected 10 targets to further investigate the

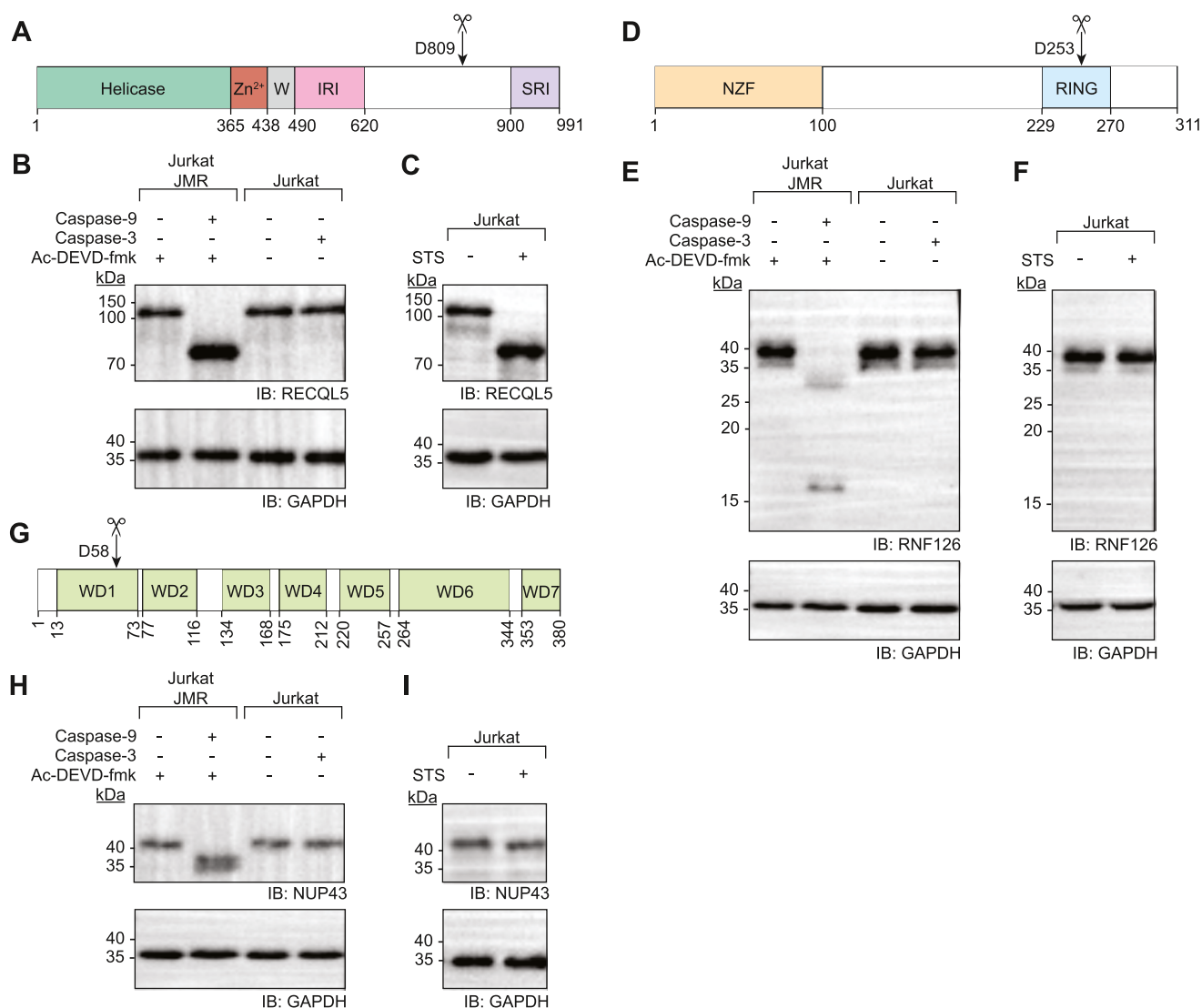


Figure 4. RECQL5, RNF126, and NUP43 are the substrates of caspase-9 but not of caspase-3. STS-induced apoptosis results in the proteolysis of RECQL5 but not RNF126 and NUP43. (A) Domain organization of RECQL5 comprises a helicase domain, zinc-binding domain, wedge domain, IRI domain, internal RNAPII-interacting domain, and SRI domain, set2-Rpb1-interacting domain. Caspase-9 cleaves at D809 (N-terminomics). (B) RECQL5 is cleaved by recombinant caspase-9 but not by caspase-3. (C) Treating Jurkat cells with 0.5 μ M of STS for 3 h revealed that RECQL5 is proteolyzed during apoptosis. (D) RNF126 comprises a NZF domain, N-terminal zinc finger domain, and RING (really interesting new gene) domain. Caspase-9 cleaves at D253 (N-terminomics). (E) RNF126 is cleaved by recombinant caspase-9 but not by caspase-3. (F) RNF126 is not cleaved during STS-induced apoptosis suggesting that caspase-9 has a putative non-apoptotic role. (G) NUP43 has seven WD40 repeat (also known as Trp–Asp 40 repeat) domains. Caspase-9 cleaves at D58 (N-terminomics). (H) NUP43 is cleaved by recombinant caspase-9 but not by caspase-3. (I) NUP43 is not cleaved during STS-induced apoptosis suggesting that caspase-9 has a putative non-apoptotic role. As a loading control, each immunoblot was stripped using a stripping buffer and then immunoblotted using an anti-GAPDH antibody. Each experiment was performed twice using two different samples on two different days (see Figure S8 for the second replicate).

cleavage sites we observed (Table 1). The intention in selecting these 10 targets was to pick a mixture of cleavage sites within and outside the DegraBase. Some of these cleavage sites were observed only in the caspase-3 experiments, some only in the caspase-9 experiments, and some in both experiments. The aim of these studies is to further understand the unique and overlapping roles of these caspases. We also sought to probe in detail substrates featuring multiple caspase cleavage sites. Moreover, for diversification, we selected substrates that belong to different functional protein families: a DNA helicase, three E3 ubiquitin ligases, a nucleoporin, a pore-forming membrane protein, a GTPase, a kinase, a ribonuclease, and a protein involved in RNA processing. It is important to mention

that we reported here all of our validation attempts and did not withhold any data.

Caspase-9 Cleaves Distinct Substrates from Caspase-3. As mentioned above, of the 124 caspase-9 substrates observed, 50 of them (43%) were not observed in the caspase-3 experiment (Figure 3C), although these experiments were run using the same protocol. For further investigation into novel roles of caspase-9, we selected three caspase-9 substrates that are not cleaved by caspase-3: ATP-dependent DNA helicase Q5 (RECQL5), nucleoporin 43 (NUP43), and E3 ubiquitin–protein ligase–ring finger protein 126 (RNF126).

RECQL5 is a DNA helicase involved in chromosomal and genome stability, DNA replication, and double strand break repair.^{52–54} The full-length RECQL5 can be divided into two

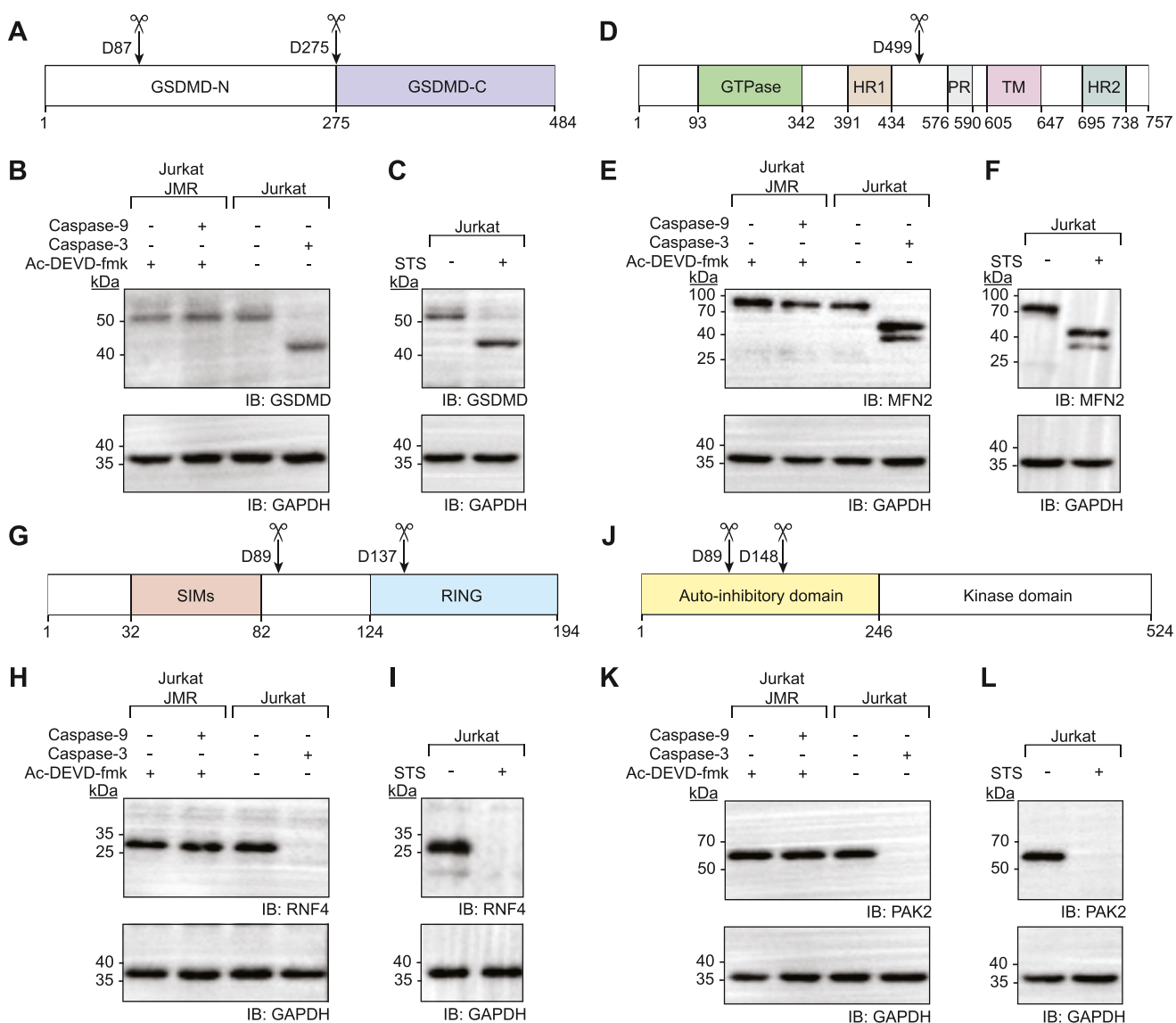


Figure 5. GSDMD, MFN2, RNF4, and PAK2 are the substrates of caspase-3 but not of caspase-9 and are proteolyzed during STS-induced apoptosis. (A) GSDMD is composed of two domains: GSDMD-N (N-terminal domain also known as a pore-forming domain) and GSDMD-C (CTD also known as an autoinhibitory domain). N-terminomics reveals caspase-3 cleavage at D87 and D275. (B) GSDMD is cleaved by recombinant caspase-3 but not by caspase-9. (C) Jurkat cells treated with 0.5 μ M of STS for 3 h revealed that GSDMD is proteolyzed during apoptosis. (D) MFN2 has a GTPase domain, HR1 (first coiled-coil heptad-repeat region), PR (proline-rich) domain, TM (transmembrane) domain, and HR2 (second coiled-coil heptad-repeat region) domain. N-terminomics revealed caspase-3 cleavage at D499. (E) MFN2 is cleaved by recombinant caspase-3 but not by caspase-9. (F) MFN2 is cleaved during STS-induced apoptosis. (G) RNF4 has four tandem SIMs (SUMO-interaction motifs) in the N-terminal domain between residues 32–82 and a RING domain at the C-terminal. N-terminomics revealed caspase-3 cleavage at D89 and D137. (H) RNF4 is cleaved by recombinant caspase-3 but not by caspase-9. (I) RNF4 is cleaved during STS-induced apoptosis. (J) PAK2 is composed of two domains: autoinhibitory (regulatory) and kinase domains. N-terminomics revealed caspase-3 cleavage at D89 and D148. (K) Immunoblot analysis resembled N-terminomics data that PAK2 is cleaved by recombinant caspase-9 but not by caspase-3. (L) PAK2 is proteolyzed during STS-induced apoptosis. As a loading control, each immunoblot was stripped using a stripping buffer and then immunoblotted using an anti-GAPDH antibody. Each experiment was performed twice using two different samples on two different days (see Figure S9 for the second replicate).

parts: the N-terminal region (primarily responsible for helicase activity) composed of a helicase domain, a zinc-binding domain, a wedge domain, and the C-terminal region (mainly involved in DNA repair during transcription) containing an internal Pol II-interacting (IRI) domain and a Set2-Rpb1-interacting (SRI) domain (Figure 4A).⁵⁵ As was observed in our N-terminomics experiments, RECQL5 was robustly cleaved in Jurkat cell lysates treated with caspase-9 but not with caspase-3 (Figure 4B). Importantly, RECQL5 was also cleaved in Jurkat cells treated with the general kinase inhibitor

and apoptosis inducer, STS, which led to expected phenotypic changes associated with apoptosis (Figure 4C). From our N-terminomics data, caspase-9 cleaves RECQL5 at D809 removing the SRI domain (Table 1 and Figure 4A). To maintain genome stability, the SRI domain of RECQL5 directly interacts with multiple binding partners, such as RNA polymerase I,⁵⁶ RNA polymerase II,^{53,57} and proliferating cell nuclear antigen.⁵⁸ Thus, caspase-9 cleavage would prevent these interactions. From our N-terminomics data, both RECQL5 and DNA topoisomerase II alpha, which is likewise

involved in DNA decatenation and cell cycle progression,⁵⁹ were observed to be cleaved by caspase-9 but not by caspase-3 (Supplemental File S1). Given the fact that the cell cycle, DNA replication, and DNA repair should be halted in the initial stage of apoptosis, our results suggest that caspase-9 also cleaves critical early apoptotic substrates. These data strongly suggested that caspase-9 can act as an executioner, and its role is not limited to only serve as an initiator of apoptosis through cleavage of caspase-3 and -7.

RNF126 is an E3 ubiquitin ligase known to target the p21 tumor suppressor and as such is considered a potentially useful cancer biomarker or therapeutic target.^{60,61} RNF126 possesses two domains, an N-terminal zinc finger domain⁶² and a C-terminal RING (really interesting new gene) domain (Figure 4D).⁶¹ RNF126 was readily identified in the caspase-9 N-terminomics analysis; however, it was neither found as a caspase-3 substrate in our analysis nor in the DegraBase (Table 1). Consistent with the N-terminomics findings, RNF126 was cleaved by caspase-9 but not by caspase-3 (Figure 4E). In addition, when apoptosis was induced by STS, no RNF126 cleavage was observed (Figure 4F). Thus, RNF126 could be a new non-apoptotic substrate of caspase-9. One of the known functions of RNF126 is that its RING domain directly interacts and ubiquitinates activation-induced cytidine deaminase (AICDA), an enzyme that deaminates deoxycytidines in single-stranded DNA.⁶³ The exact outcome of this ubiquitination (whether AICDA is degraded or not) remains to be determined *in vivo*. AICDA is predominantly expressed in germinal centers, and as an immune response, it produces and distributes high affinity antibodies against foreign antigens.⁶⁴ Because caspase-9 cleaves RNF126 in the RING domain at D253 (Table 1 and Figure 4D), this cleavage is likely to disrupt the ability of RNF126 to ubiquitinate AICDA.

While a number of nucleoporins have previously been reported as caspase substrates,^{65,66} NUP43, a component of the nucleoporin complex (NPC), was also identified as a new substrate of caspase-9 that had not been observed in previous studies. Cleavage of nucleoporins is critical as it allows entry of caspases lacking a nuclear localization signal into the nucleus.⁶⁷ NUP43 is composed of seven WD40 repeat domains, WD1 to WD7 (Figure 4G).⁶⁸ Although caspase-9 was robustly able to cleave NUP43 in Jurkat cell lysates, no cleavage by caspase-3 was observed (Figure 4H). These findings are consistent with our N-terminomics analyses (Table 1). In contrast, when apoptosis was induced by STS, no NUP43 cleavage was observed (Figure 4I) suggesting that NUP43 is not an apoptotic substrate cleaved in STS-treated cells. Induction of apoptosis by etoposide has been previously shown to result in cleavage of other nucleoporins including NUP93 and NUP96 but also did not result in cleavage of NUP43.⁶⁹ This provides increased evidence that NUP43 could be a substrate of caspase-9 under non-apoptotic conditions. The caspase-9 cleavage of NUP43 occurs in the WD1 domain at D58 (Table 1 and Figure 4G). In the NPC, NUP43 has been shown to interact with other nucleoporins, NUP85 and Seh1.^{68,70} Therefore, it remains to be discovered how the overall structure and function of NPC are changed upon caspase-9 cleavage of NUP43.

Majority of Caspase-3 Substrates are Not Recognized by Caspase-9. Of the 906 substrate proteins cleaved by caspase-3 in our analysis, 832 of the proteins were not cleaved by caspase-9. We selected four unique caspase-3 substrates for further analysis: GSDMD, mitofusin 2 (MFN2), E3 ubiquitin—

protein ligase—RING finger protein 4 (RNF4), and serine/threonine protein kinase PAK 2 (PAK2). All of these substrates were also cleaved at the expected sites when apoptosis was initiated by STS in Jurkat cells (Figure 5), strongly suggesting that these proteins are bonafide apoptotic caspase-3 substrates.

GSDMD, a pore-forming membrane protein, controls membrane permeabilization during pyroptosis.⁷¹ GSDMD is composed of two domains, GSDMD-N (N-terminal pore-forming domain) and GSDMD-C (C-terminal autoinhibitory domain) (Figure 5A). The full-length GSDMD remains inactive by an autoinhibitory mechanism due to the presence of GSDMD-C.^{72–74} To induce pyroptosis, GSDMD is recognized by the inflammatory caspases (caspase-1, -4, -5, and -11) which cleave a linker between GSDMD-N and GSDMD-C at D275.³⁵ This cleavage facilitates GSDMD-N domains to oligomerize and form pores in the cell membrane.^{73,74} In contrast, prior work has shown that GSDMD is readily cleaved by caspase-3 in GSDMD-N at D87,⁷⁵ instead of D275.⁷⁶ Cleavage of GSDMD-N at D87 by caspase-3/-7 is critical for faithful execution of apoptosis, as it is sufficient to prevent pyroptosis.⁷⁶ Our N-terminomics data sets showed that GSDMD can be cleaved by caspase-3 at both D87 and D275, consistent with both sites reported in the DegraBase (Table 1). Mirroring the N-terminomics results, we also observed cleavage of GSDMD in Jurkat lysates incubated with caspase-3 but not with caspase-9 (Figures 5B and 57). However, the presence of a cleavage product at 43 kDa suggest that D87 is the main caspase-3 cleavage site. As expected, GSDMD was also proteolyzed in a similar manner during STS-induced apoptosis (Figure 5C).

MFN2 is present in the outer mitochondrial membrane and is essential for fusion of mitochondria.⁷⁷ MFN2 has also been implicated in the regulation of mitochondrial metabolism,⁷⁸ apoptosis,⁷⁹ shape of other organelles (e.g., endoplasmic reticulum),⁸⁰ and cell cycle progression.⁸¹ MFN2 possesses a GTPase domain, a first coiled-coil heptad-repeat region domain, a proline-rich domain, transmembrane domains, and a second coiled-coil heptad-repeat region domain (Figure 5D).⁸² MFN2 is cleaved by caspase-3 but not by caspase-9 (Table 1 and Figure 5E). Cleavage of MFN2 in Jurkat cells after induction of apoptosis (Figure 5F) further suggests that MFN2 is a bonafide apoptotic substrate solely of caspase-3, although this cleavage has not been previously reported in earlier studies (Table 1). Caspase-3 cleaves MFN2 at D499 (Table 1 and Figure 5D). This cleavage severs the GTPase domain from the second coiled-coil heptad-repeat region domain, important components of MFN2 required to initiate and induce the fusion of mitochondria (Figure 5G).^{83–85} Thus, caspase-3 cleavage of MFN2 can prevent mitochondrial fusion. Another role of MFN2 is that it interacts with BAX (Bcl-2-associated X protein) under non-apoptotic conditions, preventing apoptosis.⁸⁶ Furthermore, reduction of MFN2 levels has been shown to render cells more sensitive to mitochondrial Ca²⁺-dependent cell death.⁸⁷ Thus, we anticipate that caspase-3-mediated cleavage of MFN2 likewise increases the release of cytochrome *c*, evoking apoptosis.

RNF4 is an E3 ubiquitin ligase that recognizes small ubiquitin-like modifier (SUMO)-modified proteins and degrades them via ubiquitination.⁸⁸ RNF4 accumulates at the foci of DNA double-strand break repair, so its deficiency leads to increased DNA damage.⁸⁹ RNF4 can be divided into two parts: the N-terminal region possessing four tandem SUMO-

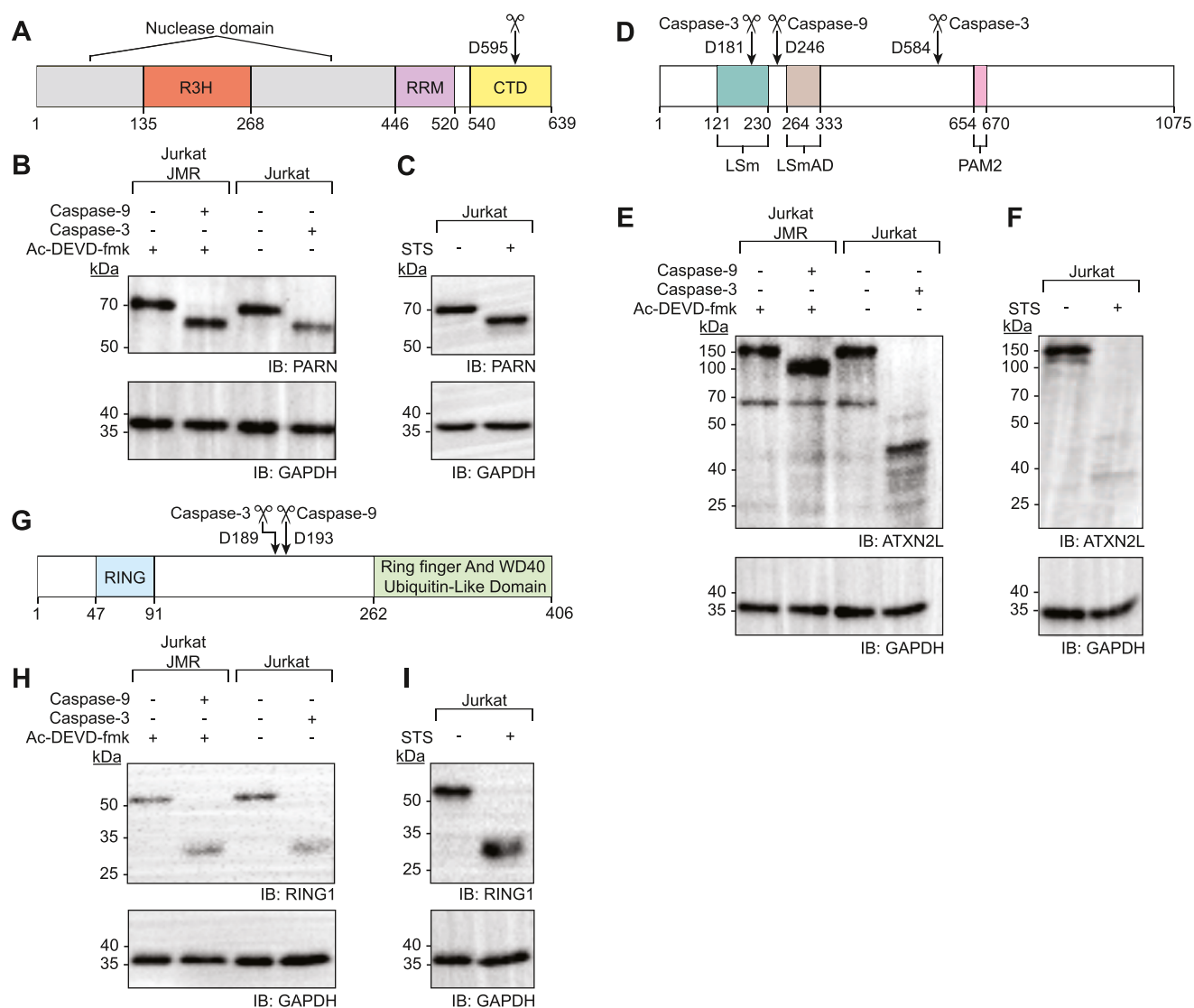


Figure 6. PARN, ATXN2L, and RING1 are the substrates of both caspase-9 and -3, and they are proteolyzed during STS-induced apoptosis. (A) PARN is composed of a catalytic nuclease domain (gray regions), R3H domain, RRM domain, and CTD. Caspase-9 cleaves at D595 (N-terminomics). (B) PARN is cleaved by recombinant caspase-9 and -3. (C) Treating Jurkat cells with 0.5 μ M of STS for 3 h revealed that PARN is proteolyzed during apoptosis. (D) ATXN2L comprises LSm, LSmAD, and PAM2 domains. N-terminomics revealed that caspase-9 cleavage occurs at D246, and caspase-3 cleavage occurs at D181 and D584. (E) ATXN2L is cleaved by recombinant caspase-9 and -3. (F) ATXN2L is cleaved during STS-induced apoptosis. (G) RING1 comprises a RING domain, a ring finger, and WD40 ubiquitin-like domain. N-terminomics revealed that caspase-9 cleavage occurs at D193, and caspase-3 cleavage occurs at D189. (H) RING1 is cleaved by recombinant caspase-9 and -3. (I) RING1 is cleaved during STS-induced apoptosis. As a loading control, each immunoblot was stripped using a stripping buffer and then immunoblotted using an anti-GAPDH antibody. Each experiment was performed twice using two different samples on two different days (see Figure S11 for the second replicate).

interacting motifs (SIMs) and the C-terminal RING domain (Figure 5G).^{90–92} We identified RNF4 as a substrate of caspase-3 but not of caspase-9 (Table 1 and Figure 5H). Moreover, RNF4 was found to be cleaved during STS-induced apoptosis in Jurkat cells (Figure 5I). RNF4 was cleaved by caspase-3 at D89 and D137 (Table 1 and Figure 5G) causing the removal of the N-terminal region that recognizes SUMO-modified proteins. The majority of SUMO-modified proteins regulated by RNF4 are involved in nucleic acid metabolism with a particular emphasis on SUMOylation, transcription, DNA repair, and chromosome segregation.⁸⁸ Since these types of cellular procedures must be halted during apoptosis, it is understandable that RNF4 emerged as an apoptotic substrate of caspase-3.

PAK2 is known to play a role in regulating apoptosis through reciprocal interactions with caspase-7.⁹³ PAK2 is composed of two domains, an autoinhibitory domain and a kinase domain (Figure 5J).^{93,94} PAK2 was identified as a substrate of caspase-3 but not of caspase-9 (Table 1 and Figure 5K). Moreover, it was proteolyzed after STS-induced apoptosis in Jurkat cells (Figure 5L). In its full-length form, PAK2 stimulates cell survival by the phosphorylation and inactivation of caspase-7.^{93,95} PAK2 is also a known substrate of caspase-3 and -7.^{93,96} Cleavage of PAK2 by caspase-3 or -7 at D212 removes the autoinhibitory domain.⁹⁴ As a result, the kinase domain translocates from the cytoplasm to the nucleus and phosphorylates a new set of substrates contributing to apoptosis.⁹⁷ Intriguingly, in the caspase-3 N-terminomics

analysis, we did not observe cleavage at D212 but rather observed two cleavages at D89 and D148 (Table 1 and Figure 5J). These results appear to be in line with our observation of PAK2 cleavage *in vitro* which demonstrates that PAK2 is such an excellent substrate of caspase-3 that it completely disappears on the immunoblot after incubation with caspase-3 (Figure 5K) and during STS-induced apoptosis (Figure 5L).

Caspase-3 and -9 Share Some Common Substrates.

Of the 906 caspase-3 substrate proteins and 124 caspase-9 substrate proteins, 74 substrate proteins were cleaved by both caspases. These 74 substrate proteins represent 57% of all caspase-9 substrate proteins identified, suggesting that there is significant redundancy between caspase-9 and -3 substrates. We selected three common substrates of caspase-3 and -9, poly(A)-specific ribonuclease (PARN), ataxin-2-like protein (ATXN2L), and E3 ubiquitin-protein ligase RING1, for further investigation.

PARN is a deadenylating nuclease that regulates mRNA turnover and non-coding RNA maturation.^{98,99} PARN possesses three well-structured RNA-binding domains [catalytic nuclease domain, an R3H domain, and an RNA recognition motif (RRM) domain]¹⁰⁰ and an intrinsically disordered C-terminal domain (CTD) (Figure 6A).^{101,102} From our N-terminomics analyses, PARN was observed to be a substrate of both caspase-3 and -9, in which both caspases cleaved PARN in the CTD at the same site, D595 (Table 1 and Figure 6A). These results mirror our immunoblotting analysis (Figure 6B). The CTD interacts with the other regions of PARN and enhances the overall thermal stability of this protein.¹⁰² Moreover, the CTD of PARN contains a nucleolar localization signal (residues: 598–624) and interacts with the nuclear non-coding RNAs in response to DNA damage.¹⁰¹ Thus, PARN cleavage by caspase-3 and -9 at D595 can not only prevent PARN access to the nucleolus but also destabilize the protein. Cleavage in the CTD appears to be crucial, as both caspase-3 and -9 execute this apoptotic role (Figure 6B), and it is cleaved during STS-induced apoptosis (Figure 6C). Deficiency in PARN leads to shortening of telomeres.¹⁰³ Thus, PARN inactivation would likewise be associated with the DNA fragmentation that is observed during apoptosis.

ATXN2L, a component of stress granules, plays a role in RNA processing and possesses three domains: like-Sm protein (LSm) domain, LSm-associated domain (LSmAD) domain, and PABP-interacting motif 2 (PAM2) domain (Figure 6D).¹⁰⁴ ATXN2L is cleaved by both caspase-3 and -9, which recognize different cleavage sites: D181 and D584 for caspase-3 and D246 for caspase-9 (Table 1 and Figure 6D). These outcomes from N-terminomics analyses mirrored our immunoblotting results (Figure 6E). Moreover, ATXN2L was readily proteolyzed during STS-induced apoptosis demonstrating that it is an apoptotic substrate (Figure 6F). ATXN2L appears to play a similar role to its paralog, ataxin-2, as it interacts with ataxin-2 itself and with ataxin-2 interacting proteins, an RNA helicase, DDX6 (perhaps through the LSm and LSmAD domains), and PABP (perhaps through the PAM2 domain).¹⁰⁴ Caspase-9 cleavage at D246 removes the LSm domain of ATXN2L (Table 1 and Figure 6D) which may prevent ATXN2L interactions with DDX6. Since caspase-3 cuts ATXN2L at two distinct sites, D181 and D584 (Table 1 and Figure 6D), these cleavages may disrupt the ability of ATXN2L to interact with DDX6 and PABP. Since RNA helicases (e.g., DDX6) are involved in the production of virtually all RNA types, targeting ATXN2L provides a means to

block RNA production and function globally in roles including translation. These analyses underscore the observation that redundancy for key apoptotic substrates (such as global regulators of RNA metabolism) may be built into multiple caspases.

RING1 (also known as RING1A) is an E3 ubiquitin ligase that we observed to be a substrate of both caspase-3 and -9, which cleave RING1 at independent sites (Table 1). RING1 is cleaved by caspase-3 at D189 and by caspase-9 at D193 (Table 1 and Figure 6G) which are both between the RING domain¹⁰⁵ and a ubiquitin-like domain.¹⁰⁶ We observed RING1 cleavage in our *in vitro* cleavage assay for both caspase-3 and -9, correlating with our N-terminomics data (Figure 6H). RING1 is known to degrade p53 protein causing proliferation of cancerous cells.¹⁰⁷ For this reason, RING1 is perhaps an unsurprising apoptotic substrate (Figure 6I). Caspase cleavage of RING1 should protect p53 from degradation, resulting in the needed ability to induce apoptosis. RING2 (also known as RING1B), which is highly homologous to RING1, was reported as a direct substrate of caspase-3 (cleaves at D175) and caspase-9 (cleaves at D208).²⁵ Interestingly, these cleavages are also occurring between the RING domain and the ubiquitin-like domain of RING2. These cleavages by caspase-3 and -9 lead to the redistribution of RING2 from nuclear localization to even distribution throughout the entire cell.²⁵ The N-terminomics identification of RING1, as a substrate of caspase-3 and -9 (cleaving at different sites), may suggest that RING1 cleavage may lead to similar impacts on cellular localization. As was the case for ATXN2L, it is tempting to speculate that a key role for RING1 in apoptosis led to the evolution of cleavage sites for redundant cleavage by both caspase-3 and -9. In addition, the observation that these two caspases cleave at different sites within the same local region (D189/193) further underscores the importance of this cleavage event, perhaps even under different mechanisms of cell death that engage caspases uniquely.

DISCUSSION

In this study, we sought to discover and compare all possible caspase substrates cleaved by the executioner caspase-3 and the initiator caspase-9. We report 906 and 124 putative protein substrates targeted by caspase-3 and caspase-9, respectively. Of the 124 caspase-9 substrates, 50 of them were not observed in the caspase-3 experiment. Our results clearly show that caspase-3 and caspase-9 possess both common and distinct pools of protein substrates. We found that some of these substrates are cleaved during apoptosis, while others are not, suggesting new non-apoptotic roles in the biology of these two caspases.

A strength of the reverse N-terminomics approach is that it allows identification of new substrates that could not be identified by other means. GSDMD, MFN2, RNF4, and PAK2 are all substrates of caspase-3 but not of caspase-9 (Table 1 and Figure 5). Neither RNF4 nor MFN2 had been observed as apoptotic substrates previously. GSDMD was cleaved by caspase-3 (Table 1 and Figure 5) and showed the detectable cleavage product in apoptotic cells (Figure 5), consistent with the DegraBase. In our immunoblot analyses, full-length PAK2 and RNF4 were fully degraded when incubated with caspase-3 and during STS-induced apoptosis. No cleavage products were observed (Figure 5), suggesting that caspase-3 likely disrupts the antibody epitope for detection. We likewise interrogated three unique caspase-9 substrates, RECQL5, NUP43, and

RNF126. We observed RECQL5 proteolysis during STS-induced apoptosis but no cleavage of NUP43 and RNF126 (Figure 4), indicating that caspase-9 plays putative non-apoptotic roles involving these substrates. Detection of PARN, ATXN2L, and RING1 as the common substrates of caspase-3 and -9 again illustrates advantages of employing reverse N-terminomics. Both ATXN2L and RING1 were reported as apoptotic substrates in the DegraBase; nonetheless, it is our reverse N-terminomics analyses which revealed that they are proteolyzed by caspase-3 and -9, at distinct cleavage sites. Our analyses also discovered new caspase cleavage sites for these three substrates, PARN (D595 by caspase-3 and -9), two additional cleavage sites of ATXN2L (D181 by caspase-3 and D246 by caspase-9), and one additional cleavage site of RING1 (D189 by caspase-9) (Table 1). Together these observations underscore the complementarity of both forward and reverse N-terminomics experiments to capture the nuanced suite of substrates of these proteases.

The comprehensive list of caspase-3 and caspase-9 substrates we provide here allowed us to finally deorphanize more than a thousand caspase substrates (Supplemental File S1). Not surprisingly, hundreds of them have been identified before as apoptotic substrates (649 out of 906 for caspase-3 and 103 out of 124 for caspase-9). However, until now, it was unknown which caspase was most responsible for these proteolytic events. Not surprisingly, the executioner caspase-3 cleaves hundreds of apoptotic substrates. The fact that prior studies did not identify any caspase-9 substrates,¹⁶ and our literature search only found seven non-caspase substrates,^{20–25} our work in deorphanizing more than hundred caspase-9 substrates represents a significant milestone in the field of caspase-9 biology. Our findings clearly demonstrate that the role of caspase-9 is not only to activate caspase-3 and -7 but also to target its own set of protein substrates.

We curated the caspase-9 substrate list, searching the literature for any references to caspase or apoptosis. Of the 124 substrate proteins (137 cleavage sites) from N-terminomics, we found the literature references for only 28 proteins which are reported as caspase substrates and/or are involved in apoptosis (Table S1). In contrast, of those 124 caspase-9 substrates, only 20 were not in the DegraBase,¹⁵ which catalogues apoptotic substrates derived from 33 different experiments ranging over seven different apoptosis inducers in five independent cell lines, reporting a total of 1706 cleavage sites in 1268 proteins. Thus, most of the caspase-9 substrates identified in this study (84%) are, in fact, apoptotic substrates that were orphaned prior to this work. It is possible or even likely that proteolysis of the 20 proteins that were not found in the DegraBase is mediated by caspase-9 in a non-apoptotic context. Of those 20 proteins that were not found in the DegraBase (Supplemental File S1), references in the literature were present for only four substrates (ATP-dependent DNA helicase Q5, chromosome transmission fidelity protein 18 homolog, synapse associated protein 1, and PARN) as a caspase substrate and/or involved in apoptosis (Table S1), underscoring the fact that this analysis had contributed to identify 16 entirely new caspase substrates which are proteolyzed by caspase-9 (Table S2).

The discovery and deorphanization of more than a hundred new caspase-9 substrates provide a critical repository of information of other functions that caspase-9 activation plays, in addition to its role as a canonical apoptotic initiator. Interestingly, caspase-9 has been implicated in a non-apoptotic

form of cell death, called paraptosis.³⁹ Paraptosis, an apaf-1-independent but caspase-9-dependent form of programmed cell death, was first termed over two decades ago, which can occur during development and neurodegeneration.³⁹ It was shown that human insulin-like growth factor I receptor stimulates paraptosis in HEK293T cells and in mouse embryonic fibroblasts.³⁹ Caspase-9, but not caspase-3/-7, was also shown to play a non-apoptotic role in primitive erythropoiesis.¹⁰⁸ Thus, it is possible that some of the caspase-9 substrates we identified play crucial roles in non-apoptotic pathways such as paraptosis and/or primitive erythropoiesis.

We also investigated 74 substrates that were cleaved by both caspase-3 and caspase-9. These proteins were cleaved at the same site by both caspases in 45% of the cases, whereas 55% were cleaved at different sites. Among those 74 substrates, 35 were cleaved at just one site by caspase-3, whereas 29 were cleaved at two sites and 10 were cleaved at three or more sites (such as enhancer of mRNA-decapping protein 4, which is cleaved at six sites). In contrast, 64 of the overlapping 74 substrates were cleaved at just one site by caspase-9, whereas nine substrate were cleaved at two sites and only one substrate (U2 snRNP-associated SURP motif-containing protein) was cleaved at four sites. The canonical view is that caspase cleavage at a single site leads to changes in function or localization that contribute to apoptosis. The observation of large numbers of cleavage sites in a single substrate begs the question of whether caspases play degradative roles for some key substrates.

We also observed that multiple members of the same functional complex are often targeted by caspases. For example, it is been shown that the proteasome, the condensin I complex, and the spliceosome are heavily targeted by caspases during apoptosis.^{26,109} Consistently, we found an enrichment for RNA splicing in both sets of caspase-3 and caspase-9 substrates. We also found that caspase-3 and caspase-9 can cleave the same substrate in the same region but at different aspartate residues (e.g., RING1 is cleaved at D189 by caspase-9 and at D193 by caspase-3). Similarly, synapse associated protein 1 (SYAP1) was shown to be cleaved by caspase-1 at D278 and by caspase-3 and -7 at D281, with a cleavage site motif, FVSD²⁷⁸↓AFD²⁸¹↓A.³² Interestingly, in this study, we found that SYAP1 is also cleaved by caspase-9 at the same site at caspase-1 (D278). We hypothesize that this redundancy, cleavage by different caspases that function in different biological pathways at adjacent and therefore likely functionally similar sites, may provide a means of identifying proteolytic events that are critical in multiple contexts.

To conclude, our study has deorphanized hundreds of caspase-3 and -9 protein substrates. Most of these proteolytic events obviously play key roles in apoptosis, induced by caspase-3 and/or caspase-9 proteolysis. However, we anticipate that these data sets will provide a powerful resource for the future investigation of the roles of these caspases in apoptotic and non-apoptotic pathways.

■ MATERIALS AND METHODS

DNA Plasmids. The expression construct for WT caspase-3 (pET23b-Casp3-His)¹¹⁰ was a gift from Guy Salvesen and obtained from Addgene (plasmid 11821). The expression construct for WT caspase-9 (pET23b-Casp9-His)¹¹¹ was a gift from Guy Salvesen and obtained from Addgene (plasmid 11829). The expression constructs

for subtiligase expression (WT and M222A mutants) were a gift from Jim Wells and Amy Weeks.⁴³

Protein Expression and Purification. Recombinant His-tagged caspase-3 was expressed in BL21 (DE3) pLysS *E. coli*. One colony was added to 50 mL of 2×YT media supplemented with ampicillin and chloramphenicol. The following morning, 25 mL of the starter culture was used to inoculate 3 L of 2×YT (Fisher Scientific) supplemented with 100 μg/mL ampicillin and 12.5 μg/mL chloramphenicol at 37 °C until the O.D. of 0.6 was reached. We then induced expression for 5 h at 30 °C using 0.3 mM IPTG (Fisher Scientific). Cells pellets were collected by centrifugation of the culture at 4000g for 20 min at 4 °C. The supernatant was discarded, and the pellet was frozen at −80 °C. The following day, the pellet was thawed on ice and resuspended in 45 mL of lysis buffer (100 mM NaCl and 100 mM Tris, pH 8.0). Cells were lysed through high-pressure homogenization (Avestin Emulsiflex C3), then centrifuged at 40,000g for 45 min at 4 °C. The clarified protein supernatant was passed through a 1 mL Ni²⁺ affinity column (Cytiva Inc.), following which protein was eluted from the column using a linear gradient (elution buffer: 500 mM NaCl, 20 mM imidazole, and 100 mM Tris, pH 8.0). The eluted protein purity was confirmed via SDS-PAGE. Eluted fractions were pooled and buffer exchanged through size exclusion chromatography (HiLoad 16/600 Superdex 200 pg, Cytiva Inc.), eluting in storage buffer (100 mM NaCl, 25 mM Tris, pH 7.5, and 2 mM DTT). Fractions were assayed for DEVDase activity. The fractions with the highest activity were pooled and concentrated using a 10 K MWCO filter spin concentrator (Cytiva Inc.).

The DNA plasmid encoding caspase-9 was transformed into BL21 (DE3) T7 express strain of *E. coli* (New England Biolabs) and plated on a LB+agar Petri dish to grow overnight at 37 °C. We picked a single colony and transferred it into a flask containing 50 mL of LB media (Research Products International). We incubated this media at 37 °C overnight to grow a seed culture. Next day, we diluted 1 mL of the seed culture one thousand times using 1 L of LB media containing 0.1 mg/mL ampicillin (Fisher BioReagents). We incubated this culture at 37 °C until the desired O.D. of 1.0 is obtained. We induced the culture by adding IPTG (GoldBio) to a final concentration of 1 mM and lowered the temperature to 25 °C for 4 h. We centrifuged this culture at 5000g for 7 min at 4 °C, and cell pellets were collected and stored at −80 °C until their use for purification. The frozen pellet was thawed and diluted in 200 mL of lysis buffer (50 mM sodium phosphate, pH 7.0, 300 mM NaCl, 5% glycerol, and 2 mM imidazole). Cells were lysed using a microfluidizer (Microfluidics, Inc.), and cell lysate was separated from the cell debris by centrifugation at 50,000g for 1 h at 4 °C. Cell lysis was purified using a Hi-Trap chelating HP column charged with Ni²⁺ (Cytiva Inc.). We performed a linear gradient (0–33% of elution buffer) and eluted protein using an elution buffer (50 mM sodium phosphate, pH = 7.0, 300 mM NaCl, 5% glycerol, and 300 mM imidazole). Eluted protein was diluted five times using buffer A (20 mM Tris, pH 8.5, 5% glycerol, and 2 mM DTT). Then, for further purification by anion exchange chromatography, we applied protein to the Hi-Trap Q HP column (Cytiva Inc.). The column was washed and then developed with a linear gradient (0–30% of buffer B: 20 mM Tris, pH 8.5, 1 M NaCl, 5% glycerol, and 2 mM DTT). Purity and concentration of purified caspase-9 were assessed using SDS-PAGE. The most concentrated fractions were aliquoted to store at −80 °C for further usage.

Mammalian Cell Culture. Jurkat cells were used for caspase-3 experiments, while Jurkat JMR (caspase-9 knockout) were used for caspase-9 experiments.⁴⁴ Caspase activity was assayed in lysate compared to buffer (Figures S1 and S2) (see caspase activity assays *in vitro* and in cell lysate for detailed procedures). Jurkat and Jurkat JMR cell pellets were thawed from frozen stocks and grown in RPMI cell culture media (Gibco), supplemented with 10% fetal bovine serum (Sigma Inc.), 100 μg/mL penicillin/streptomycin (Gibco), and 2 mM L-glutamine (Gibco). Cells were grown at 37 °C, passing stepwise from growing in culture dishes to 4 L spinner flasks. Cells were harvested by centrifugation at 800g for 5 min, washed with cold PBS,

and centrifuged again at 800g for 5 min. Pellets were kept frozen at −80 °C until required for reverse N-terminomics experiments.

Caspase Activity Assays *In Vitro* and in Cell Lysate. The caspase-3 activity in cell lysates was monitored over the course of the N-terminomics experiment by measuring DEVDase activity using an Ac-DEVD-afc fluorogenic probe (excitation/emission at 400 nm/505 nm). This assay was initiated upon addition of 0.5 μM of recombinant caspase-3 to the Jurkat lysate. Aliquots were removed and assayed at 5 min, 1, and 2 h (see caspase-3 reverse N-terminomics for lysate preparation conditions).

We analyzed the LEHDase activity of caspase-9 *in vitro* (activity assay buffer: 100 mM MES, pH 6.5, and 10 mM DTT) to optimize the concentration needed for cell lysate experiments. Caspase-9 concentrations ranging from 0 to 15 μM were prepared in a 96-well black plate using activity assay buffer. We immediately transferred 3 mM of the caspase-9 fluorogenic peptide substrate, Ac-LEHD-afc (Enzo Life Sciences, Inc.). The lowest concentration at which we observed an acceptable signal to noise ratio was 8 μM of caspase-9; therefore, we used that concentration for all subsequent assays performed in cell lysates. We lysed 2.4 × 10⁶ Jurkat JMR cells using a lysis buffer [5 mM EDTA, 1 mM PMSF, 4 mM iodoacetamide (IAM), 1 mM AEBSF, and 0.1% Triton X-100 in 100 mM HEPES, pH 7.4] on ice for 30 min. Cell lysate was separated from cell debris by centrifugation at 4000g for 15 min. Then, cell lysate was incubated with 8 μM of caspase-9 in activity assay buffer for 4 h. Meanwhile, we examined LEHDase activity of caspase-9 in cell lysate at 0, 0.5, 1, 2, and 4 h. To quench DEVDase activity (i.e., expected to be generated by an activation of endogenous caspase-3/-7 by added recombinant caspase-9), we supplemented the lysis buffer with 25 μM Ac-DEVD-fmk (Enzo Life Sciences, Inc.) and then examined both DEVDase and LEHDase activity.

Caspase-3 Reverse N-Terminomics Lysate Preparation. 7.5 × 10⁸ harvested Jurkat cells were thawed on ice and resuspended in lysis buffer (5 mM EDTA, 1 mM PMSF, 4 mM IAM, 1 mM AEBSF, and 0.1% Triton X-100 in 100 mM HEPES, pH 7.4). The sample was incubated for 45 min in the dark at room temperature, then sonicated using a probe tip sonicator at 20% amplitude, 2 s on 5 s off for 5 min. 20 mM DTT was added to quench the IAM, to retain the activity of the caspase-3 that is added subsequently. The total protein concentration in the cell lysate was determined to be 7 mg/mL using a Bradford assay kit (Bio-Rad Laboratories). The lysate was centrifuged for 10 min at 4000g to remove cell debris. A concentrated caspase activity buffer (10×) was added to the lysate (for final concentrations of 10 mM HEPES, pH 7.4, 50 mM KCl, 1.5% sucrose, 0.1% CHAPS, and 10 mM DTT). Lysates were incubated with 0.5 μM caspase-3 in the dark at room temperature for 2 h and assayed for DEVDase activity. After 2 h had elapsed, enzyme activity was irreversibly inhibited by treating with 100 μM z-VAD-fmk which quantitatively blocks the function of all caspases. We then proceeded with N-terminomics labeling (see below).

Caspase-9 Reverse N-Terminomics Lysate Preparation. We grew and harvested 5 × 10⁸ of Jurkat JMR cells. To lyse the cells, we directly suspended the cell pellet (without freezing) in a lysis buffer (100 mM HEPES, pH 7.4, 5 mM EDTA, 1 mM PMSF, 4 mM IAM, 1 mM AEBSF, 25 μM Ac-DEVD-fmk, and 0.1% Triton X-100) and then incubated on ice in the dark for 30 min. The total protein concentration in the cell lysate was determined to be 10 mg/mL using a BCA assay kit (ThermoFisher Scientific). We added 20 mM of DTT to the cell lysate to quench the IAM. The lysate was centrifuged for 10 min at 4000g to remove cell debris. A concentrated caspase-9 activity assay buffer (for final concentrations of 100 mM MES, pH = 6.5, and 10 mM DTT) was added to the lysate, following which 8 μM purified caspase-9 was added. Lysates were incubated with caspase-9 in the dark at room temperature for 4 h and assayed for LEHDase activity. Then, the enzyme activity in treated lysates was irreversibly inhibited by treating with 100 μM z-VAD-fmk. We stored this sample at −80 °C for the further usage in reverse N-terminomics.

Caspase-3 and -9 Reverse N-Terminomics. Lysates were incubated with 1 mM TEVest6 biotin peptide ester tag⁴³ and subtiligase (1 μM wild-type and 1 μM M222A mutant)⁴³ for 2 h.

Labeling was monitored by immunoblot using a streptavidin IRDye 800CW (LI-COR Inc.) (Figure S3). Protein was precipitated in acetonitrile at $-20\text{ }^{\circ}\text{C}$ overnight. The precipitate was recovered by centrifugation at 12,000g, resuspended in 8 M guanidine hydrochloride, and boiled with 100 mM tris(2-carboxyethyl)phosphine for 15 min. Once cooled, resuspension was treated with 4 mM IAM and incubated in the dark for 1 h. The sample was then reduced with 20 mM DTT and precipitated in ethanol (100 proof) at $-80\text{ }^{\circ}\text{C}$ overnight. The following morning, the precipitate was recovered by centrifugation and resuspended in 8 M guanidine hydrochloride, which was diluted to 4 M with water once the precipitate was dissolved. Neutravidin agarose beads were added to the resuspension and incubated overnight at room temperature on a rotator. Capture efficiency was measured by dot blot using the same streptavidin IRDye 800CW (Figure S3). When a 90% capture efficiency was observed, the beads were washed with a biotin wash solution (1 mM biotin, 10 mM bicine, pH 8.0), washed with 4 M guanidine hydrochloride, and then washed and resuspended in a trypsin buffer (100 mM bicine, pH 8.0, 200 mM NaCl, 20 mM CaCl_2 , and 1 M guanidine hydrochloride). 20 μg of trypsin (Promega) was added and incubated overnight at room temperature on a rotator. The next day, the trypsin in buffer was washed from the beads using 4 M guanidine hydrochloride. The neutravidin beads were then resuspended in TEV protease buffer (100 mM ammonium bicarbonate, pH 8.0, 2 mM DTT, and 1 mM EDTA). 65 μM TEV protease was added to the resuspension before they were incubated overnight at room temperature on a rotator. The next day, the supernatant was recovered and dried on a Genevac solvent evaporator (SP Scientific). When dried, the samples were resolubilized in 5% trifluoroacetic acid and incubated for 10 min at room temperature to precipitate the TEV protease. Samples were centrifuged, and the supernatant was desalted using C18 desalting resin tips (PureSpeed Rainin). The eluted solution from the desalting was dried on a Genevac.

Mass Spectrometry. Dried samples were resuspended in 10 μL of 0.1% formic acid. Peptides were analyzed using a nanoflow-HPLC (Thermo Scientific EASY-nLC 1000 system) coupled to a Lumos (Thermo Fisher Scientific) mass spectrometer. Peptides were eluted using a 120 min 0–42% linear acetonitrile gradient, followed by elution with 80% acetonitrile. Data were analyzed using ProteinProspector (v5.22.1) software against the human proteome (2017-11-01 human proteome sequence downloaded from <https://www.uniprot.org>). Search parameters included non-tryptic cleavage at N-termini, missed trypsin cleavages, and precursor and mass tolerance, as detailed in Supplemental File S1 for each data set. Variable modifications such as carbamidomethylation of Cys, oxidation of Met, deamidation of Asn and Gln, and addition of abu were searched, as detailed in Supplemental File S1. The TEVest6 biotin ester peptide tag contains an unnatural residue, abu that is retained on labeled peptides following TEV protease cleavage of peptides from the neutravidin beads. Search parameters included a strict false discovery rate of 5% for proteins and 1% for peptides. The maximum number of variable modifications was set to two. Data including peak lists are available on the MS-viewer repository (<https://prospector.uclsf.edu>) with search keys mdjft1fbxv (caspase-3, replicate 1), lltypq1rr0 (caspase-3, replicate 2), 65spzmsu6p (caspase-9, replicate 1), and xcn4gexgdo (caspase-9, replicate 2). Raw files can be found in the massIVE repository: MSV000087447 (caspase-3, both replicates) and MSV000087448 (caspase-9, both replicates).

Sample Preparation for Immunoblotting. For the cleavage assays using recombinant caspase-3 and -9, we followed the same procedure to prepare the samples for immunoblotting as we did for reverse N-terminomics. After the incubation with the respective caspase (or only buffer A without caspase as a control) and addition of z-VAD-fmk, we added 1 \times SDS blue loading dye (New England Biolabs) and denatured the samples by heating at $90\text{ }^{\circ}\text{C}$ for 10 min. Samples were aliquoted and stored at $-80\text{ }^{\circ}\text{C}$ until the further usage.

For STS-induced apoptosis assays, we treated Jurkat cells (5×10^7) with either 0.5 μM of STS or dimethyl sulfoxide (control). We incubated these cultures at $37\text{ }^{\circ}\text{C}$ for 3 h to induce apoptosis. Then, we lysed cells following the same protocol as for N-terminomics. At

last, we added 1 \times SDS blue loading dye (New England Biolabs) and denatured the samples by heating at $90\text{ }^{\circ}\text{C}$ for 10 min. These samples were also aliquoted and stored at $-80\text{ }^{\circ}\text{C}$ until further usage.

Immunoblotting Analysis. The samples were thawed, and the proteins were separated by molecular weight using gel electrophoresis. We used a 12% SDS-PAGE gel for RECQL5, GSDMD, MFN2, PAK2, PARN, and ATXN2L and a 16% SDS-PAGE gel for NUP43, RNF126, RNF4, and RING1. The proteins were transferred from the SDS-PAGE gel to an immobilon-P PVDF membrane (MilliporeSigma). These membranes were washed five times with TBST over a period of 30 min. The membranes were then blocked using OneBlock Western-CL Blocking Buffer (Genesee Scientific Corporation) at $4\text{ }^{\circ}\text{C}$ for 1 h. Primary antibody solutions were prepared as follows: RECQL5 [ThermoFisher Scientific (PA5-56315); final concentration: 0.1 $\mu\text{g}/\text{mL}$], NUP43 [ThermoFisher Scientific (A303-976A); 1:5000 dilution], RNF126 [abcam (ab183102); 1:700 dilution], GSDMD [MilliporeSigma (G7422); 1:1000], MFN2 [abcam (ab205236); 1:5000 dilution], RNF4 [R&D Systems (AF7964); final concentration: 1 $\mu\text{g}/\text{mL}$], PAK2 [Cell Signaling Technology (2608); 1:5000 dilution], PARN [abcam (ab188333); 1:5000 dilution], ATXN2L [Proteintech Group, Inc. (24822-1-AP); 1:5000 dilution], and RING1 [Cell Signaling Technology (13069); 1:5000 dilution] into 10 mL of blocking buffer. After removing the blocking buffer from the membranes, they were incubated with primary antibodies solutions at $4\text{ }^{\circ}\text{C}$ overnight. The next day, the membranes were washed five times with TBST over a period of 30 min and subsequently incubated with secondary antibodies: RNF4, rabbit anti-goat IgG HRP antibody [R&D Systems (HAF017); 1:10,000 dilution], and for all the other antibodies, goat anti-rabbit IgG H L HRP [Genesee Scientific Corporation (20–303); 1:10,000 dilution]. The incubation for secondary antibodies was performed for 1 h, and then, the membranes were washed five times using a TBST buffer over the period of 30 min. At last, the signal was detected using a SuperSignal West Dura Extended Duration Substrate kit (ThermoFisher Scientific). The images of immunoblots were taken using a ChemiDoc MP imaging system (Bio-Rad Laboratories) and analyzed using Image Lab software (Bio-Rad Laboratories). GAPDH protein levels were used as a loading control. Each membrane was stripped by incubating with a mild stripping buffer (1.5% glycine, pH 2.2, 0.1% SDS, and 1% Tween 20) for 10 min. The membranes were washed twice with PBS and then twice with TBST and incubated with GAPDH primary antibody [ThermoFisher Scientific (MAS-15738); 1:5000 dilution] and secondary antibody, goat anti-mouse IgG H L HRP [Genesee Scientific Corporation (20–304); 1:10,000 dilution], as described above.

■ ASSOCIATED CONTENT

Supporting Information

The Supporting Information is available free of charge at <https://pubs.acs.org/doi/10.1021/acscchembio.1c00456>.

Activity assay, enhanced N-terminomics bioinformatic analysis, immunoblots (duplicates), and LC–MS/MS data (PDF)

Complete lists of caspase-3 and -9 substrates (XLSX)

■ AUTHOR INFORMATION

Corresponding Author

Olivier Julien – Department of Biochemistry, University of Alberta, Edmonton T6G 2H7 Alberta, Canada;
orcid.org/0000-0001-7068-7299; Email: ojulien@ualberta.ca

Authors

Luam E. Araya – Department of Biochemistry, University of Alberta, Edmonton T6G 2H7 Alberta, Canada;
orcid.org/0000-0003-1991-3443

Ishankumar V. Soni – Department of Chemistry, University of Massachusetts, Amherst 01003 Massachusetts, United States
Jeanne A. Hardy – Department of Chemistry, University of Massachusetts, Amherst 01003 Massachusetts, United States
✉ orcid.org/0000-0002-3406-7997

Complete contact information is available at:
<https://pubs.acs.org/10.1021/acscchembio.1c00456>

Author Contributions

[§]These authors contributed equally to this work.

Notes

The authors declare no competing financial interest.

ACKNOWLEDGMENTS

We thank G. Salvesen, S. Snipas, A. Mahar, and G. Baron for helpful discussions and J. Moore for technical support and maintaining the mass spectrometers. We received funding from Alberta Innovates (L.A.) and the Natural Sciences and Engineering Research Council of Canada (discovery grant to O.J. and CGSM to L.A.). I.V.S. was supported in part by NIH GM T32 GM008515. This work was supported by NIH GM 008532. Figure 1 was adapted from “Apoptosis extrinsic and intrinsic pathways,” [BioRender.com](https://www.biorender.com) (2021).

REFERENCES

- (1) Lamkanfi, M.; Declercq, W.; Kalai, M.; Saelens, X.; Vandenabeele, P. Alice in caspase land. A phylogenetic analysis of caspases from worm to man. *Cell Death Differ.* **2002**, *9*, 358–361.
- (2) Thornberry, N. A.; Lazebnik, Y. Caspases: enemies within. *Science* **1998**, *281*, 1312–1316.
- (3) Fernando, P.; Kelly, J. F.; Balazsi, K.; Slack, R. S.; Megeney, L. A. Caspase 3 activity is required for skeletal muscle differentiation. *Proc. Natl. Acad. Sci. U. S. A.* **2002**, *99*, 11025–11030.
- (4) Lamkanfi, M.; Festjens, N.; Declercq, W.; Berghe, T. V.; Vandenabeele, P. Caspases in cell survival, proliferation and differentiation. *Cell Death Differ.* **2007**, *14*, 44–55.
- (5) Graham, R. K.; Ehrnhoefer, D. E.; Hayden, M. R. Caspase-6 and neurodegeneration. *Trends Neurosci.* **2011**, *34*, 646–656.
- (6) Stennicke, H. R.; Renatus, M.; Meldal, M.; Salvesen, G. S. Internally quenched fluorescent peptide substrates disclose the substrate preferences of human caspases 1, 3, 6, 7 and 8. *Biochem. J.* **2000**, *350*, 563–568.
- (7) Thornberry, N. A.; Rano, T. A.; Peterson, E. P.; Rasper, D. M.; Timkey, T.; Garcia-Calvo, M.; Houtzager, V. M.; Nordstrom, P. A.; Roy, S.; Vaillancourt, J. P.; Chapman, K. T.; Nicholson, D. W. A Combinatorial Approach Defines Specificities of Members of the Caspase Family and Granzyme B. *J. Biol. Chem.* **1997**, *272*, 17907–17911.
- (8) Pop, C.; Salvesen, G. S. Human caspases: activation, specificity, and regulation. *J. Biol. Chem.* **2009**, *284*, 21777–21781.
- (9) Denecker, G.; Hoste, E.; Gilbert, B.; Hochepeid, T.; Ovaere, P.; Lippens, S.; Van den Broecke, C.; Van Damme, P.; D’Herde, K.; Hachem, J.-P.; Borgonie, G.; Presland, R. B.; Schoonjans, L.; Libert, C.; Vandekerckhove, J.; et al. Caspase-14 protects against epidermal UVB photodamage and water loss. *Nat. Cell Biol.* **2007**, *9*, 666–674.
- (10) Elmore, S. Apoptosis: a review of programmed cell death. *Toxicol. Pathol.* **2007**, *35*, 495–516.
- (11) Li, P.; Nijhawan, D.; Budihardjo, I.; Srinivasula, S. M.; Ahmad, M.; Alnemri, E. S.; Wang, X. Cytochrome c and dATP-dependent formation of Apaf-1/caspase-9 complex initiates an apoptotic protease cascade. *Cell* **1997**, *91*, 479–489.
- (12) Denault, J.-B.; Salvesen, G. S. Human caspase-7 activity and regulation by its N-terminal peptide. *J. Biol. Chem.* **2003**, *278*, 34042–34050.
- (13) Soni, I. V.; Hardy, J. A. Caspase-9 Activation of Procaspase-3 but Not Procaspase-6 Is Based on the Local Context of Cleavage Site Motifs and on Sequence. *Biochemistry* **2021**, *60* (37), 2824–2835.
- (14) Fulda, S.; Debatin, K.-M. Extrinsic versus intrinsic apoptosis pathways in anticancer chemotherapy. *Oncogene* **2006**, *25*, 4798–4811.
- (15) Crawford, E. D.; Seaman, J. E.; Agard, N.; Hsu, G. W.; Julien, O.; Mahrus, S.; Nguyen, H.; Shimbo, K.; Yoshihara, H. A. L.; Zhuang, M.; Chalkley, R. J.; Wells, J. A. The DegraBase: a database of proteolysis in healthy and apoptotic human cells. *Mol. Cell. Proteomics* **2013**, *12*, 813–824.
- (16) Agard, N. J.; Mahrus, S.; Trinidad, J. C.; Lynn, A.; Burlingame, A. L.; Wells, J. A. Global kinetic analysis of proteolysis via quantitative targeted proteomics. *Proc. Natl. Acad. Sci. U. S. A.* **2012**, *109*, 1913–1918.
- (17) Srinivasula, S. M.; Ahmad, M.; Fernandes-Alnemri, T.; Alnemri, E. S. Autoactivation of procaspase-9 by Apaf-1-mediated oligomerization. *Mol. Cell* **1998**, *1*, 949–957.
- (18) Slee, E. A.; Harte, M. T.; Kluck, R. M.; Wolf, B. B.; Casiano, C. A.; Newmeyer, D. D.; Wang, H.-G.; Reed, J. C.; Nicholson, D. W.; Alnemri, E. S.; Green, D. R.; Martin, S. J. Ordering the cytochrome c-initiated caspase cascade: hierarchical activation of caspases-2, -3, -6, -7, -8, and -10 in a caspase-9-dependent manner. *J. Cell Biol.* **1999**, *144*, 281–292.
- (19) McComb, S.; Chan, P. K.; Guinot, A.; Hartmannsdottir, H.; Jenni, S.; Dobay, M. P.; Bourquin, J.-P.; Bornhauser, B. C. Efficient apoptosis requires feedback amplification of upstream apoptotic signals by effector caspase-3 or -7. *Sci. Adv.* **2019**, *5*, No. eaau9433.
- (20) Nakanishi, K.; Maruyama, M.; Shibata, T.; Morishima, N. Identification of a caspase-9 substrate and detection of its cleavage in programmed cell death during mouse development. *J. Biol. Chem.* **2001**, *276*, 41237–41244.
- (21) Ohsawa, S.; Hamada, S.; Asou, H.; Kuida, K.; Uchiyama, Y.; Yoshida, H.; Miura, M. Caspase-9 activation revealed by semaphorin 7A cleavage is independent of apoptosis in the aged olfactory bulb. *J. Neurosci.* **2009**, *29*, 11385–11392.
- (22) Duclos, C. M.; Champagne, A.; Carrier, J. C.; Saucier, C.; Lavoie, C. L.; Denault, J.-B. Caspase-mediated proteolysis of the sorting nexin 2 disrupts retromer assembly and potentiates Met/hepatocyte growth factor receptor signaling. *Cell Death Discovery* **2017**, *3*, 16100.
- (23) Grossi, S.; Fenini, G.; Kockmann, T.; Hennig, P.; Di Filippo, M.; Beer, H.-D. Inactivation of the Cytoprotective Major Vault Protein by Caspase-1 and -9 in Epithelial Cells during Apoptosis. *J. Invest. Dermatol.* **2020**, *140*, 1335–1345.
- (24) Scott, F. L.; Fuchs, G. J.; Boyd, S. E.; Denault, J.-B.; Hawkins, C. J.; Dequiedt, F.; Salvesen, G. S. Caspase-8 cleaves histone deacetylase 7 and abolishes its transcription repressor function. *J. Biol. Chem.* **2008**, *283*, 19499–19510.
- (25) Wong, C. K.; Chen, Z.; So, K. L.; Li, D.; Li, P. Polycomb group protein RING1B is a direct substrate of Caspases-3 and -9. *Biochim. Biophys. Acta* **2007**, *1773*, 844–852.
- (26) Mahrus, S.; Trinidad, J. C.; Barkan, D. T.; Sali, A.; Burlingame, A. L.; Wells, J. A. Global sequencing of proteolytic cleavage sites in apoptosis by specific labeling of protein N termini. *Cell* **2008**, *134*, 866–876.
- (27) Gevaert, K.; Goethals, M.; Martens, L.; Van Damme, J.; Staes, A.; Thomas, G. R.; Vandekerckhove, J. Exploring proteomes and analyzing protein processing by mass spectrometric identification of sorted N-terminal peptides. *Nat. Biotechnol.* **2003**, *21*, 566–569.
- (28) Kleifeld, O.; Doucet, A.; auf dem Keller, U.; Prudova, A.; Schilling, O.; Kainthan, R. K.; Starr, A. E.; Foster, L. J.; Kizhakkedathu, J. N.; Overall, C. M. Isotopic labeling of terminal amines in complex samples identifies protein N-termini and protease cleavage products. *Nat. Biotechnol.* **2010**, *28*, 281–288.
- (29) Griswold, A. R.; Cifani, P.; Rao, S. D.; Axelrod, A. J.; Miele, M. M.; Hendrickson, R. C.; Kentsis, A.; Bachovchin, D. A. A Chemical Strategy for Protease Substrate Profiling. *Cell Chem. Biol.* **2019**, *26*, 901–907.

- (30) Wejda, M.; Impens, F.; Takahashi, N.; Van Damme, P.; Gevaert, K.; Vandenabeele, P. Degradomics reveals that cleavage specificity profiles of caspase-2 and effector caspases are alike. *J. Biol. Chem.* **2012**, *287*, 33983–33995.
- (31) Arnesen, T.; Van Damme, P.; Polevoda, B.; Helsens, K.; Evjenth, R.; Colaert, N.; Varhaug, J. E.; Vandekerckhove, J.; Lillehaug, J. R.; Sherman, F.; Gevaert, K. Proteomics analyses reveal the evolutionary conservation and divergence of N-terminal acetyltransferases from yeast and humans. *Proc. Natl. Acad. Sci. U. S. A.* **2009**, *106*, 8157–8162.
- (32) Agard, N. J.; Maltby, D.; Wells, J. A. Inflammatory stimuli regulate caspase substrate profiles. *Mol. Cell. Proteomics* **2010**, *9*, 880–893.
- (33) Julien, O.; Zhuang, M.; Wiita, A. P.; O'Donoghue, A. J.; Knudsen, G. M.; Craik, C. S.; Wells, J. A. Quantitative MS-based enzymology of caspases reveals distinct protein substrate specificities, hierarchies, and cellular roles. *Proc. Natl. Acad. Sci. U. S. A.* **2016**, *113*, E2001–E2010.
- (34) Hill, M. E.; MacPherson, D. J.; Wu, P.; Julien, O.; Wells, J. A.; Hardy, J. A. Reprogramming Caspase-7 Specificity by Regio-Specific Mutations and Selection Provides Alternate Solutions for Substrate Recognition. *ACS Chem. Biol.* **2016**, *11*, 1603–1612.
- (35) Shi, J.; Zhao, Y.; Wang, K.; Shi, X.; Wang, Y.; Huang, H.; Zhuang, Y.; Cai, T.; Wang, F.; Shao, F. Cleavage of GSDMD by inflammatory caspases determines pyroptotic cell death. *Nature* **2015**, *526*, 660–665.
- (36) Kayagaki, N.; Stowe, I. B.; Lee, B. L.; O'Rourke, K.; Anderson, K.; Warming, S.; Cuellar, T.; Haley, B.; Roose-Girma, M.; Phung, Q. T.; Liu, P. S.; Lill, J. R.; Li, H.; Wu, J.; Kummerfeld, S.; et al. Caspase-11 cleaves gasdermin D for non-canonical inflammasome signalling. *Nature* **2015**, *526*, 666–671.
- (37) He, W.-t.; Wan, H.; Hu, L.; Chen, P.; Wang, X.; Huang, Z.; Yang, Z.-H.; Zhong, C.-Q.; Han, J. Gasdermin D is an executor of pyroptosis and required for interleukin-1 β secretion. *Cell Res.* **2015**, *25*, 1285–1298.
- (38) Galluzzi, L.; Vitale, I.; Aaronson, S. A.; Abrams, J. M.; Adam, D.; Agostinis, P.; Alnemri, E. S.; Altucci, L.; Amelio, I.; Andrews, D. W.; Annicchiarico-Petruzzelli, M.; Antonov, A. V.; Arama, E.; Baehrecke, E. H.; Barlev, N. A.; et al. Molecular mechanisms of cell death: recommendations of the Nomenclature Committee on Cell Death 2018. *Cell Death Differ.* **2018**, *25*, 486–541.
- (39) Sperandio, S.; de Belle, I.; Bredesen, D. E. An alternative, nonapoptotic form of programmed cell death. *Proc. Natl. Acad. Sci. U. S. A.* **2000**, *97*, 14376–14381.
- (40) Yuan, J.; Najafov, A.; Py, B. F. Roles of Caspases in Necrotic Cell Death. *Cell* **2016**, *167*, 1693–1704.
- (41) Weeks, A. M.; Byrnes, J. R.; Lui, I.; Wells, J. A. Mapping proteolytic neo-N termini at the surface of living cells. *Proc. Natl. Acad. Sci. U. S. A.* **2021**, *118*, No. e2018809118.
- (42) Zhou, J.; Li, S.; Leung, K. K.; O'Donovan, B.; Zou, J. Y.; DeRisi, J. L.; Wells, J. A. Deep profiling of protease substrate specificity enabled by dual random and scanned human proteome substrate phage libraries. *Proc. Natl. Acad. Sci. U. S. A.* **2020**, *117*, 25464–25475.
- (43) Weeks, A. M.; Wells, J. A. Engineering peptide ligase specificity by proteomic identification of ligation sites. *Nat. Chem. Biol.* **2018**, *14*, 50–57.
- (44) Samraj, A. K.; Sohn, D.; Schulze-Osthoff, K.; Schmitz, I. Loss of caspase-9 reveals its essential role for caspase-2 activation and mitochondrial membrane depolarization. *Mol. Biol. Cell* **2007**, *18*, 84–93.
- (45) Colaert, N.; Helsens, K.; Martens, L.; Vandekerckhove, J.; Gevaert, K. Improved visualization of protein consensus sequences by iceLogo. *Nat. Methods* **2009**, *6*, 786–787.
- (46) Schechter, I.; Berger, A. On the size of the active site in proteases. I. Papain. *Biochem. Biophys. Res. Commun.* **1967**, *27*, 157–162.
- (47) Talanian, R. V.; Quinlan, C.; Trautz, S.; Hackett, M. C.; Mankovich, J. A.; Banach, D.; Ghayur, T.; Brady, K. D.; Wong, W. W. Substrate specificities of caspase family proteases. *J. Biol. Chem.* **1997**, *272*, 9677–9682.
- (48) Zorn, J. A.; Wolan, D. W.; Agard, N. J.; Wells, J. A. Fibrils colocalize caspase-3 with procaspase-3 to foster maturation. *J. Biol. Chem.* **2012**, *287*, 33781–33795.
- (49) Huber, K. L.; Serrano, B. P.; Hardy, J. A. Caspase-9 CARD : core domain interactions require a properly formed active site. *Biochem. J.* **2018**, *475*, 1177–1196.
- (50) Fabregat, A.; Sidiropoulos, K.; Viteri, G.; Forner, O.; Marin-Garcia, P.; Arnau, V.; D'Eustachio, P.; Stein, L.; Hermjakob, H. Reactome pathway analysis: a high-performance in-memory approach. *BMC Bioinf.* **2017**, *18*, 142.
- (51) Barkan, D. T.; Hostetter, D. R.; Mahrus, S.; Pieper, U.; Wells, J. A.; Craik, C. S.; Sali, A. Prediction of protease substrates using sequence and structure features. *Bioinformatics* **2010**, *26*, 1714–1722.
- (52) Hu, Y.; Raynard, S.; Sehorn, M. G.; Lu, X.; Bussen, W.; Zheng, L.; Stark, J. M.; Barnes, E. L.; Chi, P.; Janscak, P.; Jasin, M.; Vogel, H.; Sung, P.; Luo, G. RECQL5/RecqL5 helicase regulates homologous recombination and suppresses tumor formation via disruption of Rad51 presynaptic filaments. *Genes Dev.* **2007**, *21*, 3073–3084.
- (53) Islam, M. N.; Fox, D.; Guo, R.; Enomoto, T.; Wang, W. RecQL5 Promotes Genome Stabilization through Two Parallel Mechanisms-Interacting with RNA Polymerase II and Acting as a Helicase. *Mol. Cell. Biol.* **2010**, *30*, 2460–2472.
- (54) Hu, Y.; Lu, X.; Zhou, G.; Barnes, E. L.; Luo, G. RecqL5 plays an important role in DNA replication and cell survival after camptothecin treatment. *Mol. Cell. Biol.* **2009**, *29*, 114–123.
- (55) Andrs, M.; Hasanova, Z.; Oravetzova, A.; Dobrovolna, J.; Janscak, P. RECQ5: A Mysterious Helicase at the Interface of DNA Replication and Transcription. *Genes* **2020**, *11*, 232.
- (56) Urban, V.; Dobrovolna, J.; Hühn, D.; Fryzelkova, J.; Bartek, J.; Janscak, P. RECQ5 helicase promotes resolution of conflicts between replication and transcription in human cells. *J. Cell Biol.* **2016**, *214*, 401–415.
- (57) Kassube, S. A.; Jinek, M.; Fang, J.; Tsutakawa, S.; Nogales, E. Structural mimicry in transcription regulation of human RNA polymerase II by the DNA helicase RECQL5. *Nat. Struct. Mol. Biol.* **2013**, *20*, 892–899.
- (58) Li, M.; Xu, X.; Chang, C.-W.; Zheng, L.; Shen, B.; Liu, Y. SUMO2 conjugation of PCNA facilitates chromatin remodeling to resolve transcription-replication conflicts. *Nat. Commun.* **2018**, *9*, 2706.
- (59) Ramamoorthy, M.; Tadokoro, T.; Rybanska, I.; Ghosh, A. K.; Wersto, R.; May, A.; Kulikowicz, T.; Sykora, P.; Croteau, D. L.; Bohr, V. A. RECQL5 cooperates with Topoisomerase II α in DNA decatenation and cell cycle progression. *Nucleic Acids Res.* **2012**, *40*, 1621–1635.
- (60) Yang, X.; Pan, Y.; Qiu, Z.; Du, Z.; Zhang, Y.; Fa, P.; Gorityala, S.; Ma, S.; Li, S.; Chen, C.; Wang, H.; Xu, Y.; Yan, C.; Ruth, K.; Ma, Z.; et al. RNF126 as a Biomarker of a Poor Prognosis in Invasive Breast Cancer and CHEK1 Inhibitor Efficacy in Breast Cancer Cells. *Clin. Cancer Res.* **2018**, *24*, 1629–1643.
- (61) Zhi, X.; Zhao, D.; Wang, Z.; Zhou, Z.; Wang, C.; Chen, W.; Liu, R.; Chen, C. E3 ubiquitin ligase RNF126 promotes cancer cell proliferation by targeting the tumor suppressor p21 for ubiquitin-mediated degradation. *Cancer Res.* **2013**, *73*, 385–394.
- (62) Krysztofinska, E. M.; Martinez-Lumbreras, S.; Thapaliya, A.; Evans, N. J.; High, S.; Isaacson, R. L. Structural and functional insights into the E3 ligase, RNF126. *Sci. Rep.* **2016**, *6*, 26433.
- (63) Delker, R. K.; Zhou, Y.; Strikoudis, A.; Stebbins, C. E.; Papavasiliou, F. N. Solubility-based genetic screen identifies RING finger protein 126 as an E3 ligase for activation-induced cytidine deaminase. *Proc. Natl. Acad. Sci. U. S. A.* **2013**, *110*, 1029–1034.
- (64) Choudhary, M.; Tamrakar, A.; Singh, A. K.; Jain, M.; Jaiswal, A.; Kodgire, P. AID Biology: A pathological and clinical perspective. *Int. Rev. Immunol.* **2018**, *37*, 37–56.
- (65) Ferrando-May, E.; Cordes, V.; Biller-Ckovic, I.; Mirkovic, J.; Görlich, D.; Nicotera, P. Caspases mediate nucleoporin cleavage, but not early redistribution of nuclear transport factors and modulation of

nuclear permeability in apoptosis. *Cell Death Differ.* **2001**, *8*, 495–505.

(66) Cronshaw, J. M.; Krutchinsky, A. N.; Zhang, W.; Chait, B. T.; Matunis, M. J. Proteomic analysis of the mammalian nuclear pore complex. *J. Cell Biol.* **2002**, *158*, 915–927.

(67) Duclos, C.; Lavoie, C.; Denault, J.-B. Caspases rule the intracellular trafficking cartel. *FEBS J.* **2017**, *284*, 1394–1420.

(68) Xu, C.; Li, Z.; He, H.; Wernimont, A.; Li, Y.; Loppnau, P.; Min, J. Crystal structure of human nuclear pore complex component NUP43. *FEBS Lett.* **2015**, *589*, 3247–3253.

(69) Patre, M.; Tabbert, A.; Hermann, D.; Walczak, H.; Rackwitz, H.-R.; Cordes, V. C.; Ferrando-May, E. Caspases target only two architectural components within the core structure of the nuclear pore complex. *J. Biol. Chem.* **2006**, *281*, 1296–1304.

(70) von Appen, A.; Kosinski, J.; Sparks, L.; Ori, A.; DiGuilio, A. L.; Vollmer, B.; Mackmull, M.-T.; Banterle, N.; Parca, L.; Kastiris, P.; Buczak, K.; Mosalaganti, S.; Hagen, W.; Andres-Pons, A.; Lemke, E. A.; et al. In situ structural analysis of the human nuclear pore complex. *Nature* **2015**, *526*, 140–143.

(71) Rühl, S.; Broz, P. The gasdermin-D pore: Executor of pyroptotic cell death. *Oncotarget* **2016**, *7*, 57481–57482.

(72) Kuang, S.; Zheng, J.; Yang, H.; Li, S.; Duan, S.; Shen, Y.; Ji, C.; Gan, J.; Xu, X.-W.; Li, J. Structure insight of GSDMD reveals the basis of GSDMD autoinhibition in cell pyroptosis. *Proc. Natl. Acad. Sci. U. S. A.* **2017**, *114*, 10642–10647.

(73) Liu, Z.; Wang, C.; Rathkey, J. K.; Yang, J.; Dubyak, G. R.; Abbott, D. W.; Xiao, T. S. Structures of the Gasdermin D C-Terminal Domains Reveal Mechanisms of Autoinhibition. *Structure* **2018**, *26*, 778–784.

(74) Liu, Z.; Wang, C.; Yang, J.; Zhou, B.; Yang, R.; Ramachandran, R.; Abbott, D. W.; Xiao, T. S. Crystal Structures of the Full-Length Murine and Human Gasdermin D Reveal Mechanisms of Auto-inhibition, Lipid Binding, and Oligomerization. *Immunity* **2019**, *51*, 43–49.

(75) Rogers, C.; Fernandes-Alnemri, T.; Mayes, L.; Alnemri, D.; Cingolani, G.; Alnemri, E. S. Cleavage of DFNA5 by caspase-3 during apoptosis mediates progression to secondary necrotic/pyroptotic cell death. *Nat. Commun.* **2017**, *8*, 14128.

(76) Taabazuig, C. Y.; Okondo, M. C.; Bachovchin, D. A. Pyroptosis and Apoptosis Pathways Engage in Bidirectional Crosstalk in Monocytes and Macrophages. *Cell Chem. Biol.* **2017**, *24*, 507–514.

(77) Li, Y.-J.; Cao, Y.-L.; Feng, J.-X.; Qi, Y.; Meng, S.; Yang, J.-F.; Zhong, Y.-T.; Kang, S.; Chen, X.; Lan, L.; Luo, L.; Yu, B.; Chen, S.; Chan, D. C.; Hu, J.; et al. Structural insights of human mitofusin-2 into mitochondrial fusion and CMT2A onset. *Nat. Commun.* **2019**, *10*, 4914.

(78) Bach, D.; Pich, S.; Soriano, F. X.; Vega, N.; Baumgartner, B.; Oriola, J.; Daugaard, J. R.; Lloberas, J.; Camps, M.; Zierath, J. R.; Rabasa-Lhoret, R.; Wallberg-Henriksson, H.; Laville, M.; Palacín, M.; Vidal, H.; et al. Mitofusin-2 Determines Mitochondrial Network Architecture and Mitochondrial Metabolism. *J. Biol. Chem.* **2003**, *278*, 17190–17197.

(79) Sugioka, R.; Shimizu, S.; Tsujimoto, Y. Fzo1, a protein involved in mitochondrial fusion, inhibits apoptosis. *J. Biol. Chem.* **2004**, *279*, 52726–52734.

(80) de Brito, O. M.; Scorrano, L. Mitofusin-2 regulates mitochondrial and endoplasmic reticulum morphology and tethering: the role of Ras. *Mitochondrion* **2009**, *9*, 222–226.

(81) Chen, K.-H.; Guo, X.; Ma, D.; Guo, Y.; Li, Q.; Yang, D.; Li, P.; Qiu, X.; Wen, S.; Xiao, R.-P.; Tang, J. Dysregulation of HSG triggers vascular proliferative disorders. *Nat. Cell Biol.* **2004**, *6*, 872–883.

(82) Filadi, R.; Penden, D.; Pizzo, P. Mitofusin 2: from functions to disease. *Cell Death Dis.* **2018**, *9*, 330.

(83) Koshiba, T.; Detmer, S. A.; Kaiser, J. T.; Chen, H.; McCaffery, J. M.; Chan, D. C. Structural basis of mitochondrial tethering by mitofusin complexes. *Science* **2004**, *305*, 858–862.

(84) Cao, Y.-L.; Meng, S.; Chen, Y.; Feng, J.-X.; Gu, D.-D.; Yu, B.; Li, Y.-J.; Yang, J.-Y.; Liao, S.; Chan, D. C.; Gao, S. MFN1 structures

reveal nucleotide-triggered dimerization critical for mitochondrial fusion. *Nature* **2017**, *542*, 372–376.

(85) Qi, Y.; Yan, L.; Yu, C.; Guo, X.; Zhou, X.; Hu, X.; Huang, X.; Rao, Z.; Lou, Z.; Hu, J. Structures of human mitofusin 1 provide insight into mitochondrial tethering. *J. Cell Biol.* **2016**, *215*, 621–629.

(86) Karbowski, M.; Norris, K. L.; Cleland, M. M.; Jeong, S.-Y.; Youle, R. J. Role of Bax and Bak in mitochondrial morphogenesis. *Nature* **2006**, *443*, 658–662.

(87) Filadi, R.; Greotti, E.; Turacchio, G.; Luini, A.; Pozzan, T.; Pizzo, P. Mitofusin 2 ablation increases endoplasmic reticulum-mitochondria coupling. *Proc. Natl. Acad. Sci. U. S. A.* **2015**, *112*, E2174–E2181.

(88) Kumar, R.; González-Prieto, R.; Xiao, Z.; Verlaan-de Vries, M.; Vertegaal, A. C. O. The STUbL RNF4 regulates protein group SUMOylation by targeting the SUMO conjugation machinery. *Nat. Commun.* **2017**, *8*, 1809.

(89) Vyas, R.; Kumar, R.; Clermont, F.; Helfricht, A.; Kaley, P.; Sotiropoulou, P.; Hendriks, I. A.; Radaelli, E.; Hocheppied, T.; Blanpain, C.; Sablina, A.; van Attikum, H.; Olsen, J. V.; Jochemsen, A. G.; Vertegaal, A. C. O.; et al. RNF4 is required for DNA double-strand break repair in vivo. *Cell Death Differ.* **2013**, *20*, 490–502.

(90) Keusekotten, K.; Bade, V. N.; Meyer-Teschendorf, K.; Sriramachandran, A. M.; Fischer-Schrader, K.; Krause, A.; Horst, C.; Schwarz, G.; Hofmann, K.; Dohmen, R. J.; Praefcke, G. J. K. Multivalent interactions of the SUMO-interaction motifs in RING finger protein 4 determine the specificity for chains of the SUMO. *Biochem. J.* **2014**, *457*, 207–214.

(91) Kung, C. C.-H.; Naik, M. T.; Wang, S.-H.; Shih, H.-M.; Chang, C.-C.; Lin, L.-Y.; Chen, C.-L.; Ma, C.; Chang, C.-F.; Huang, T.-H. Structural analysis of poly-SUMO chain recognition by the RNF4-SIMs domain. *Biochem. J.* **2014**, *462*, 53–65.

(92) Liew, C. W.; Sun, H.; Hunter, T.; Day, C. L. RING domain dimerization is essential for RNF4 function. *Biochem. J.* **2010**, *431*, 23–29.

(93) Eron, S. J.; Raghupathi, K.; Hardy, J. A. Dual Site Phosphorylation of Caspase-7 by PAK2 Blocks Apoptotic Activity by Two Distinct Mechanisms. *Structure* **2017**, *25*, 27–39.

(94) Walter, B. N.; Huang, Z.; Jakobi, R.; Tuazon, P. T.; Alnemri, E. S.; Litwack, G.; Traugh, J. A. Cleavage and activation of p21-activated protein kinase gamma-PAK by CPP32 (caspase 3). Effects of autophosphorylation on activity. *J. Biol. Chem.* **1998**, *273*, 28733–28739.

(95) Li, X.; Wen, W.; Liu, K.; Zhu, F.; Malakhova, M.; Peng, C.; Li, T.; Kim, H.-G.; Ma, W.; Cho, Y. Y.; Bode, A. M.; Dong, Z.; Dong, Z. Phosphorylation of caspase-7 by p21-activated protein kinase (PAK) 2 inhibits chemotherapeutic drug-induced apoptosis of breast cancer cell lines. *J. Biol. Chem.* **2011**, *286*, 22291–22299.

(96) Rudel, T.; Bokoch, G. M. Membrane and morphological changes in apoptotic cells regulated by caspase-mediated activation of PAK2. *Science* **1997**, *276*, 1571–1574.

(97) Jakobi, R.; McCarthy, C. C.; Koepfel, M. A.; Stringer, D. K. Caspase-activated PAK-2 is regulated by subcellular targeting and proteasomal degradation. *J. Biol. Chem.* **2003**, *278*, 38675–38685.

(98) Virtanen, A.; Henriksson, N.; Nilsson, P.; Nissbeck, M. Poly(A)-specific ribonuclease (PARN): an allosterically regulated, processive and mRNA cap-interacting deadenylase. *Crit. Rev. Biochem. Mol. Biol.* **2013**, *48*, 192–209.

(99) Son, A.; Park, J.-E.; Kim, V. N. PARN and TOE1 Constitute a 3' End Maturation Module for Nuclear Non-coding RNAs. *Cell Rep.* **2018**, *23*, 888–898.

(100) He, G.-J.; Zhang, A.; Liu, W.-F.; Yan, Y.-B. Distinct roles of the R3H and RRM domains in poly(A)-specific ribonuclease structural integrity and catalysis. *Biochim. Biophys. Acta* **2013**, *1834*, 1089–1098.

(101) Duan, T. L.; He, G. J.; Hu, L. D.; Yan, Y. B. The Intrinsically Disordered C-Terminal Domain Triggers Nucleolar Localization and Function Switch of PARN in Response to DNA Damage. *Cells* **2019**, *8*, 836.

(102) He, G.-J.; Yan, Y.-B. Contributions of the C-terminal domain to poly(A)-specific ribonuclease (PARN) stability and self-association. *Biochem. Biophys. Rep.* **2019**, *18*, 100626.

(103) Tummala, H.; Walne, A.; Collopy, L.; Cardoso, S.; de la Fuente, J.; Lawson, S.; Powell, J.; Cooper, N.; Foster, A.; Mohammed, S.; Plagnol, V.; Vulliamy, T.; Dokal, I. Poly(A)-specific ribonuclease deficiency impacts telomere biology and causes dyskeratosis congenita. *J. Clin. Invest.* **2015**, *125*, 2151–2160.

(104) Kaehler, C.; Isensee, J.; Nonhoff, U.; Terrey, M.; Hucho, T.; Lehrach, H.; Krobitsch, S. Ataxin-2-like is a regulator of stress granules and processing bodies. *PLoS One* **2012**, *7*, No. e50134.

(105) Chen, J.; Xu, H.; Zou, X.; Wang, J.; Zhu, Y.; Chen, H.; Shen, B.; Deng, X.; Zhou, A.; Chin, Y. E.; Rauscher, F. J.; Peng, C.; Hou, Z. Snail recruits Ring1B to mediate transcriptional repression and cell migration in pancreatic cancer cells. *Cancer Res.* **2014**, *74*, 4353–4363.

(106) Sanchez-Pulido, L.; Devos, D.; Sung, Z. R.; Calonje, M. RAWUL: a new ubiquitin-like domain in PRC1 ring finger proteins that unveils putative plant and worm PRC1 orthologs. *BMC Genom.* **2008**, *9*, 308.

(107) Shen, J.; Li, P.; Shao, X.; Yang, Y.; Liu, X.; Feng, M.; Yu, Q.; Hu, R.; Wang, Z. The E3 Ligase RING1 Targets p53 for Degradation and Promotes Cancer Cell Proliferation and Survival. *Cancer Res.* **2018**, *78*, 359–371.

(108) Tran, H. T.; Fransen, M.; Dimitrakopoulou, D.; Van Imschoot, G.; Willemarck, N.; Vleminckx, K. Caspase-9 has a nonapoptotic function in *Xenopus* embryonic primitive blood formation. *J. Cell Sci.* **2017**, *130*, 2371–2381.

(109) Stoehr, G.; Schaab, C.; Graumann, J.; Mann, M. A SILAC-based approach identifies substrates of caspase-dependent cleavage upon TRAIL-induced apoptosis. *Mol. Cell. Proteomics* **2013**, *12*, 1436–1450.

(110) Zhou, Q.; Snipas, S.; Orth, K.; Muzio, M.; Dixit, V. M.; Salvesen, G. S. Target Protease Specificity of the Viral Serpin CrmA. *J. Biol. Chem.* **1997**, *272*, 7797–7800.

(111) Stennicke, H. R.; Deveraux, Q. L.; Humke, E. W.; Reed, J. C.; Dixit, V. M.; Salvesen, G. S. Caspase-9 can be activated without proteolytic processing. *J. Biol. Chem.* **1999**, *274*, 8359–8362.

(112) Luo, S. Y.; Araya, L. E.; Julien, O. Protease Substrate Identification Using N-terminomics. *ACS Chem. Biol.* **2019**, *14*, 2361–2371.